# Dispersive Alfvén wave turbulence and the role of self-generated temperature anisotropy

Thierry Passot, D. Laveder, L. Marradi, and Pierre-Louis Sulem
*UNS, CNRS, Observatoire de la Côte d'Azur, Nice, France*

***Workshop:***
Kinetic-scale turbulence in laboratory and space plasmas:
empirical constraints, fundamental concepts and unsolved problems

**Isaac Newton Institute for Mathematical Sciences, Cambridge**
19-23 july 2010

# Outline

- Dispersive range of MHD cascade in the solar wind
- Some results on Hall-MHD
- Importance of temperature anisotropy
- The Landau fluid model
- Validation of the model
- Properties of the linear system
- Nonlinear simulations in 1D at quasi-perpendicular angle
- Conclusion

# 1. Solar wind and magnetosheath observations

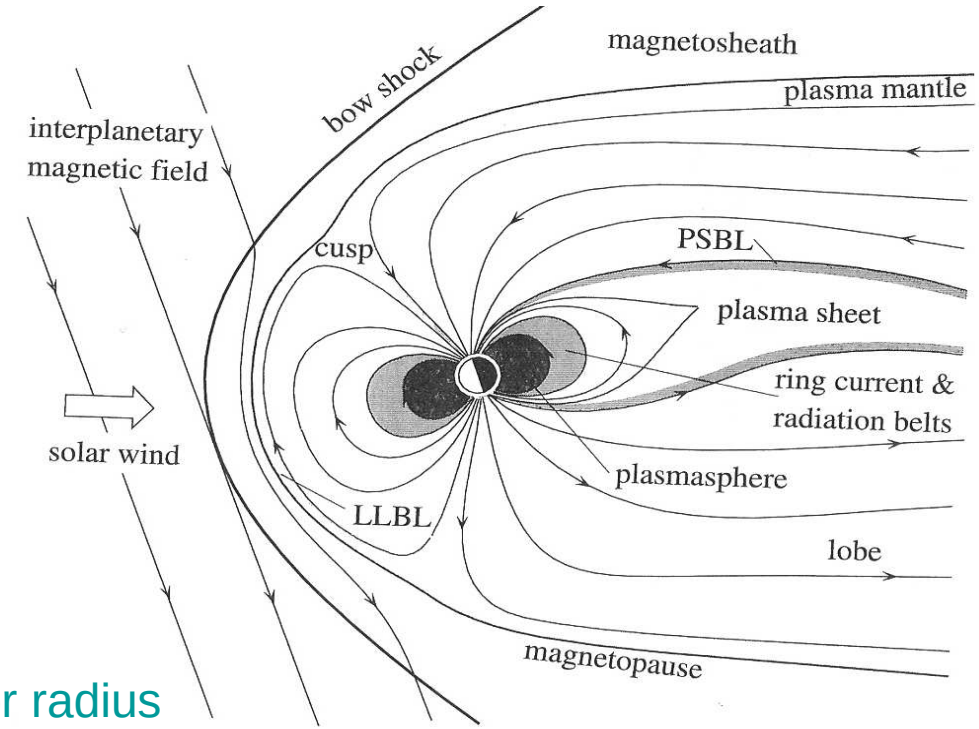


Space plasmas such as the
solar wind or the Earth magnetosheath :

- Natural laboratories for accurate in situ measurements

- Turbulent magnetized plasmas with essentially no collisions.

- Cascades extend beyond the ion Larmor radius

- Small-scale coherent structures (filaments, shocklets, magnetosonic solitons, magnetic holes) with typical scales of a few ion Larmor radius.

- Dispersive and kinetic effects play a role.

# Solar wind observations

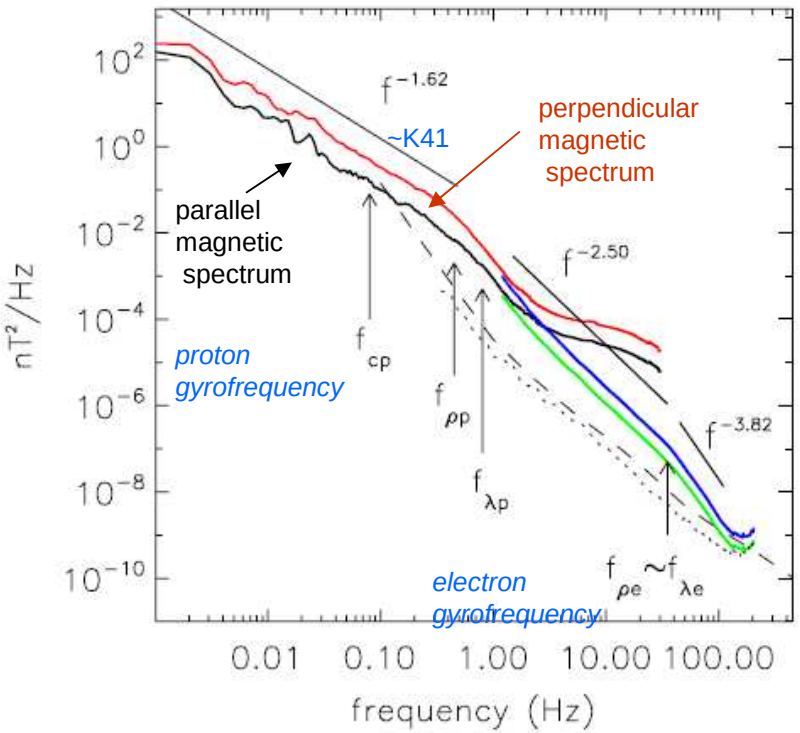


FIG. 2 (color online). The parallel (black) and perpendicular (red) magnetic spectra of FGM data ($f < 33$ Hz) and STAFF-SC data (respectively, light line; green online and dark line; blue online); $1.5 < f < 225$ Hz). The STAFF-SC noise level as measured in the laboratory and in-flight are plotted as dashed and dotted lines, respectively. The straight black lines are power law fits to the spectra. The arrows indicate characteristic frequencies defined in the text.

k-filtering -> θ=86°

*Sahraoui et al. PRL 102, 231102 (2009)*

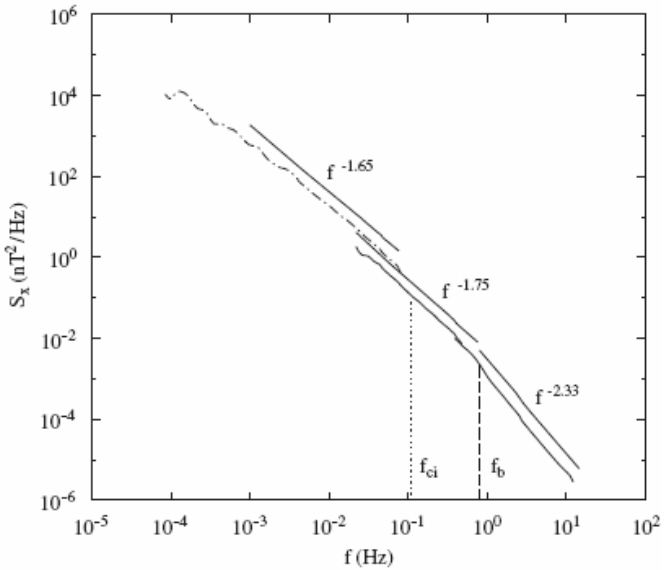


Energy spectra of $B_x$ fluctuations measured by Cluster (full line) and by Helios 2 (dashed-dotted line)

*Alexandrova et al. Planet. Space Sci. 55, 2224 (2007)*

Excess of magnetic energy in the transverse components

Does the anisotropy persist at small scales?

Several power-law ranges:

Which cascades? Which waves? Which slopes?
Important to estimate heating.
(*Ng et al. JGR 115, A02101; 2010*)

At what scale does dissipation take place?
By which mechanism?

## The simplest model beyond MHD that contains dispersive effects: Hall-MHD

$$\partial_t \rho + \nabla.(\rho \mathbf{u}) = 0$$

$$\rho(\partial_t \mathbf{u} + \mathbf{u}.\nabla \mathbf{u}) = -\frac{\beta}{\gamma}\nabla \rho^\gamma + (\nabla \times \mathbf{b}) \times \mathbf{b}$$

$$\partial_t \mathbf{b} - \nabla \times (\mathbf{u} \times \mathbf{b}) = \underbrace{-\frac{1}{R_i}\nabla \times (\frac{1}{\rho}(\nabla \times \mathbf{b}) \times \mathbf{b})}_{\text{Hall term}}$$

$$\nabla.\mathbf{b} = 0$$

velocity unit: Alfvén speed
length unit : $R_i \times$ ion inertial length
time unit: $R_i \times$ ion gyroperiod
density unit: mean density
magnetic field unit: ambient field

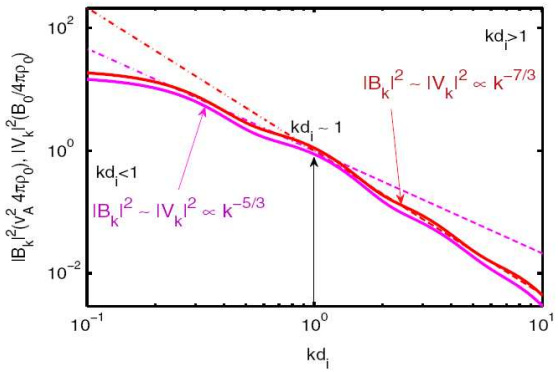


*Shaikh and Shukla, PRL 102, 045004 (2009)*

In the presence of an ambient field, the Hall term induces dispersive effects.

Hall-MHD is a rigorous limit of collisionless kinetic theory for:

$T_i << T_e$
$\omega << \Omega_i$
$k_{||} v_{thi} << \omega << k_{||} v_{the}$

*Irose et al. , Phys. Lett. A 330, 474 (2004)*
*Ito et al., PoP 11, 5643 (2004)*
*Howes, NPG 16, 219 (2009)*

It correctly reproduces whistlers and KAW's for small to moderate β.

*It contains waves that are usually damped in a collisionless plasma and whose influence in the turbulent dynamics has to be evaluated.*

## One-dimensional simulations:

Random driving (white noise in time) on the **transverse components** of velocity *(kinetic driving)* or magnetic field *(magnetic driving*).

## Questions:

- Influence of the dispersion strength (by changing the size of the domain and thus the ratio between the scale of energy injection and the ion inertial length).
- Influence of the angle of propagation.
- Influence of the type of driving (kinetic or magnetic).
- Spectral transfer versus coupling between various MHD modes.

*Laveder et al., Planet. Space Sci., in press*

# Parallel propagation, Large-scale kinetic driving

(weakly dispersive regime)

$L=16\pi\, l_i$

$K_{inj}\, d_i=1/2$

$\beta=2$

$\gamma=5/3$

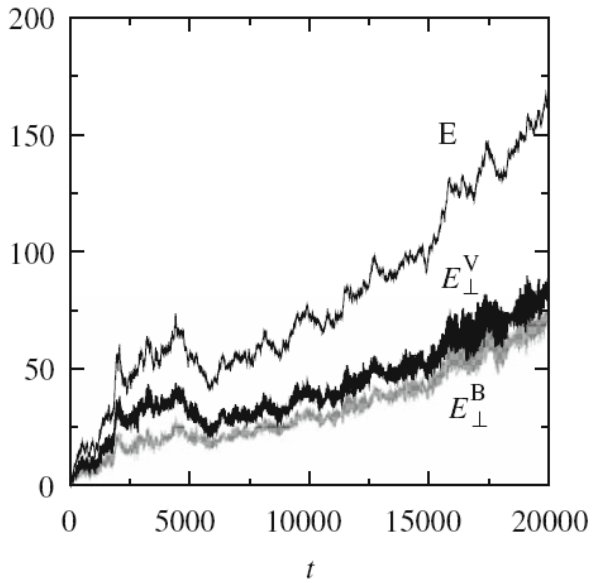


## Energy does not saturate:

significant inverse transfer

(time unit: inverse ion gyrofrequency)

## Etablishment of a pressure-balanced state

(not limited to largest scales: persists when largest scales are filtered out).

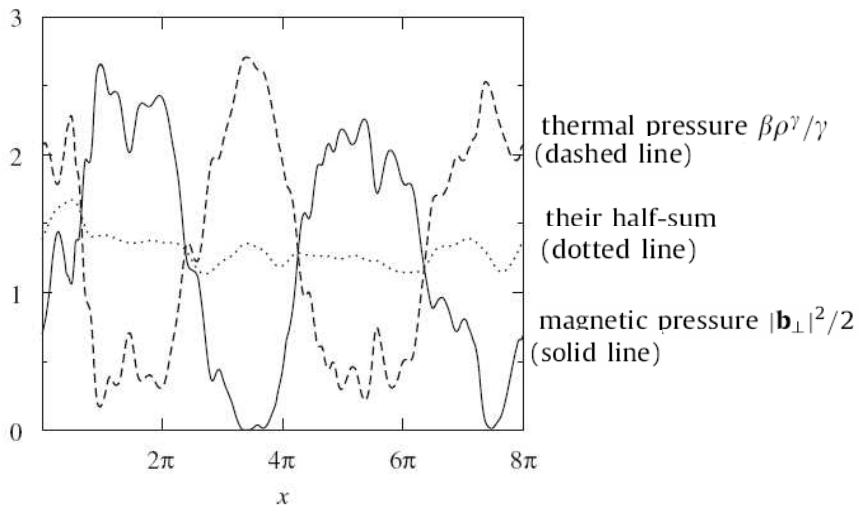


Transverse velocity $|\mathbf{v}_\perp|^2$

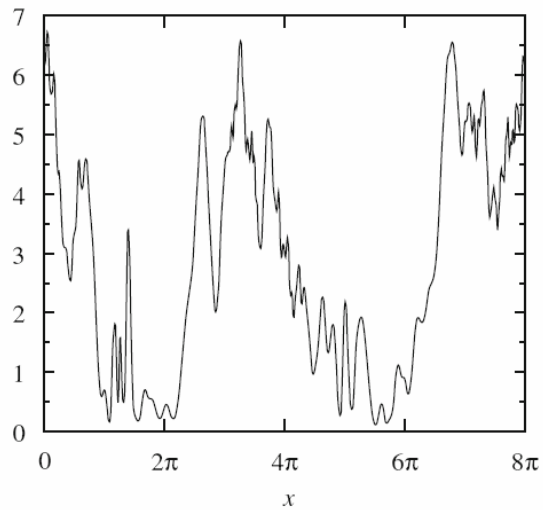


After filtering the n=1 mode

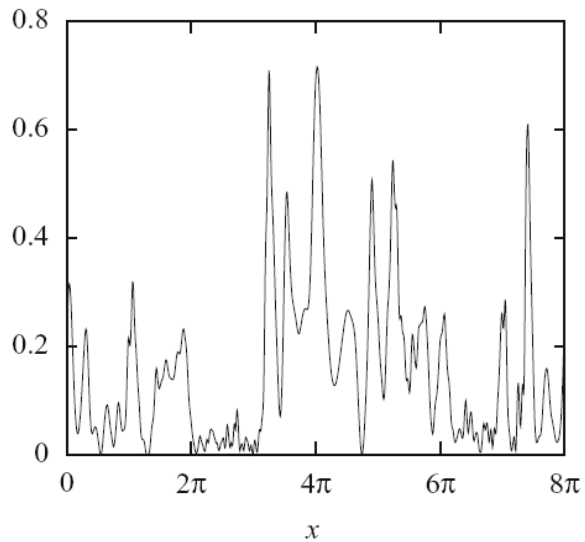


## Solitonic waves

that survive collisions

## Large-scale kinetic driving (continued)

Energy spectra: distinct power laws at large and small scales:

Transition near the ion inertial scale (consistent with solar wind observations: Leamon et al. '98, Golstein and Robert '99, Alexandrova et al. '06, Sahraoui et al. '09)

Non universal small-scale exponents
(influence of small-scale cusp-like structures and wave-packets)

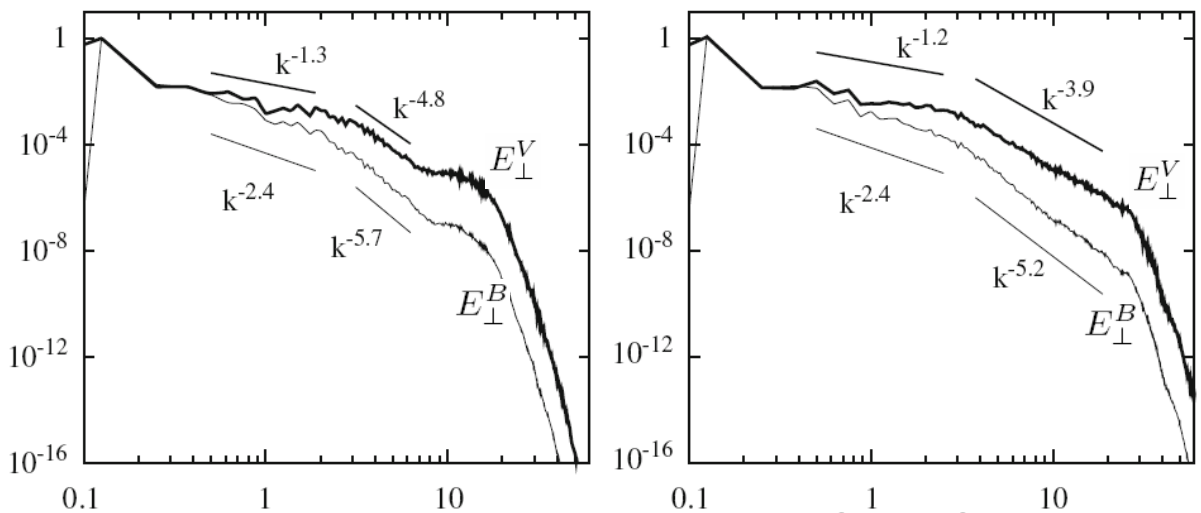


Kinetic $|\hat{\mathbf{v}}_y|^2 + |\hat{\mathbf{v}}_z|^2$ (thick line) and magnetic $|\hat{\mathbf{b}}_y|^2 + |\hat{\mathbf{b}}_z|^2$ (thin line) spectra averaged over the time interval $t = 18\,200 - 18\,250$ (left)
$t = 19\,500 - 19\,550$ (right)

Transverse kinetic spectrum shallower than the magnetic one

Dominance of kinetic on magnetic modes suggests an ion-cyclotron turbulence

## Energy dissipation affects dominantly the parallel field components

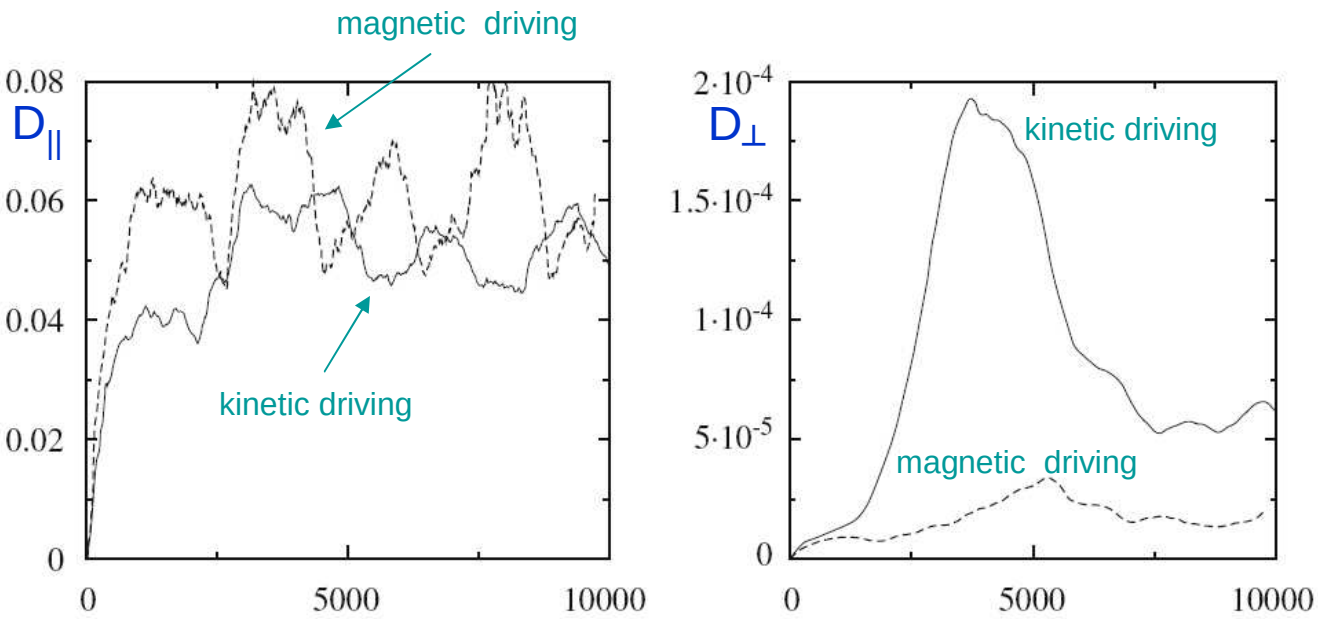


Left: time evolution of the parallel dissipation $D_{||}$ for the kinetic (solid line) and magnetic (dashed line) drivings
Right: same for the perpendicular dissipation $D_{\perp}$

In the weakly dispersive regime, injected energy is transferred to sonic waves and dissipated through a cascade of acoustic waves.

Sonic wave turbulence is the dominant phenomenon, although small scales also form on the transverse field components but on a longer time scale.

# Strongly intermittent energy transfer from Alfvén to magnetosonic waves

Instantaneous rate of energy transfer from Alfvén to magneto-sonic waves.

Instantaneous parallel dissipation

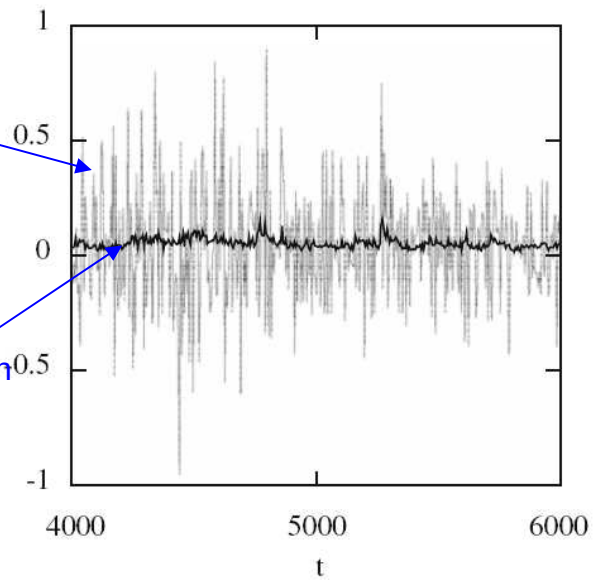


After averaging on 1000 ion gyroperiods

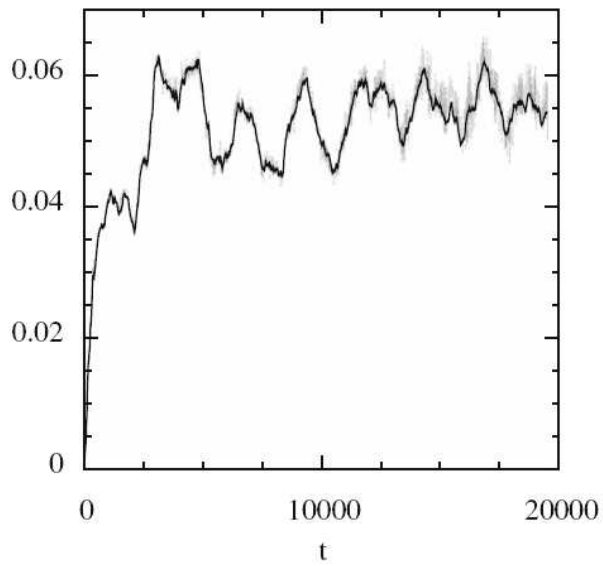


(kinetic driving)

Forcing no longer persistent but monitored to maintain a constant total energy:

In the case of a large-scale kinetic forcing (weakly dispersive regime), a spectral hole forms at intermediate scales, showing the absence of Alfvén wave cascade.

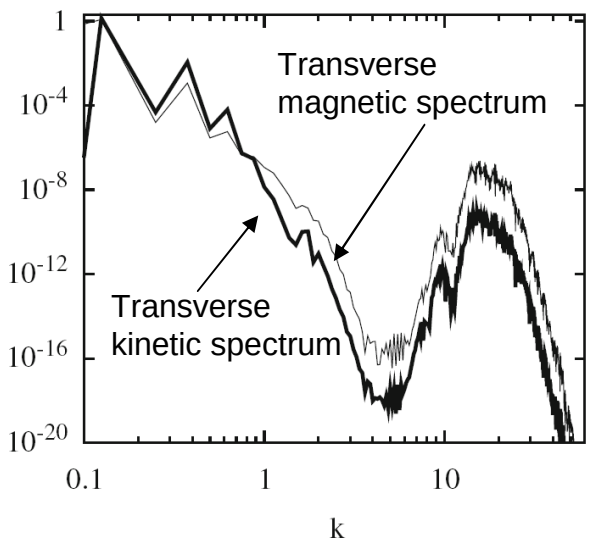


kinetic $|\hat{\mathbf{v}}_y|^2 + |\hat{\mathbf{v}}_z|^2$ (thick line) and
magnetic $|\hat{\mathbf{b}}_y|^2 + |\hat{\mathbf{b}}_z|^2$ (thin line) spectra

**Differently, in a more dispersive regime**, an Alfvén wave cascade is possible.

(qualitative agreement with weak-turbulence analysis on Vlasov equation: Yoon & Fang 2008).

No spectral gap in the case of monitored driving.

Quasi-transverse propagation

80°

Large-scale kinetic driving

(weakly dispersive regime)

Early inverse cascade that saturates

Pressure-balanced state perturbed by dispersive shocks

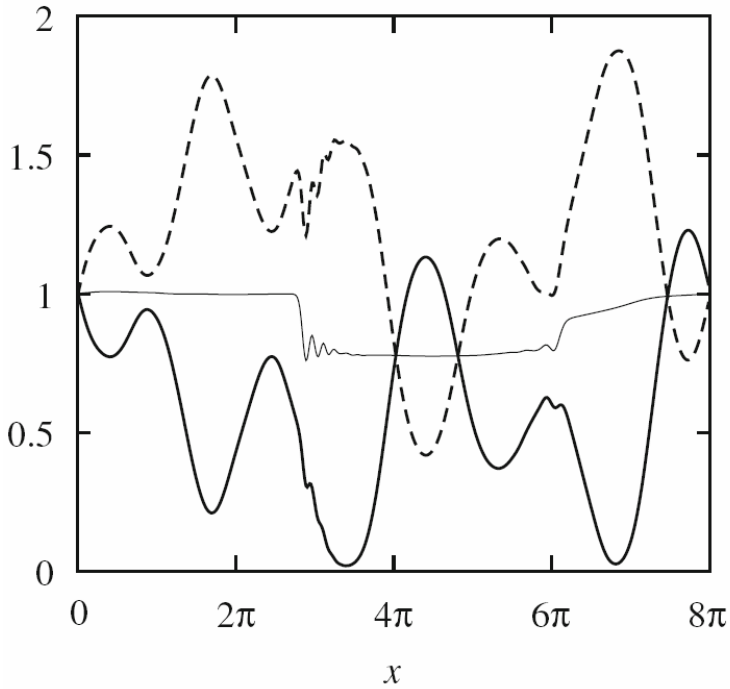


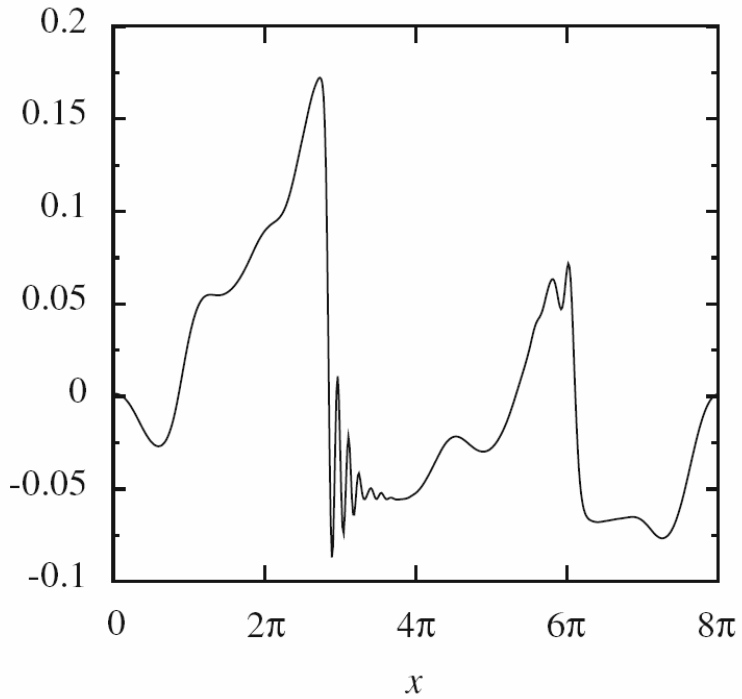

Quasi transverse propagation, weakly dispersive regime (continued):

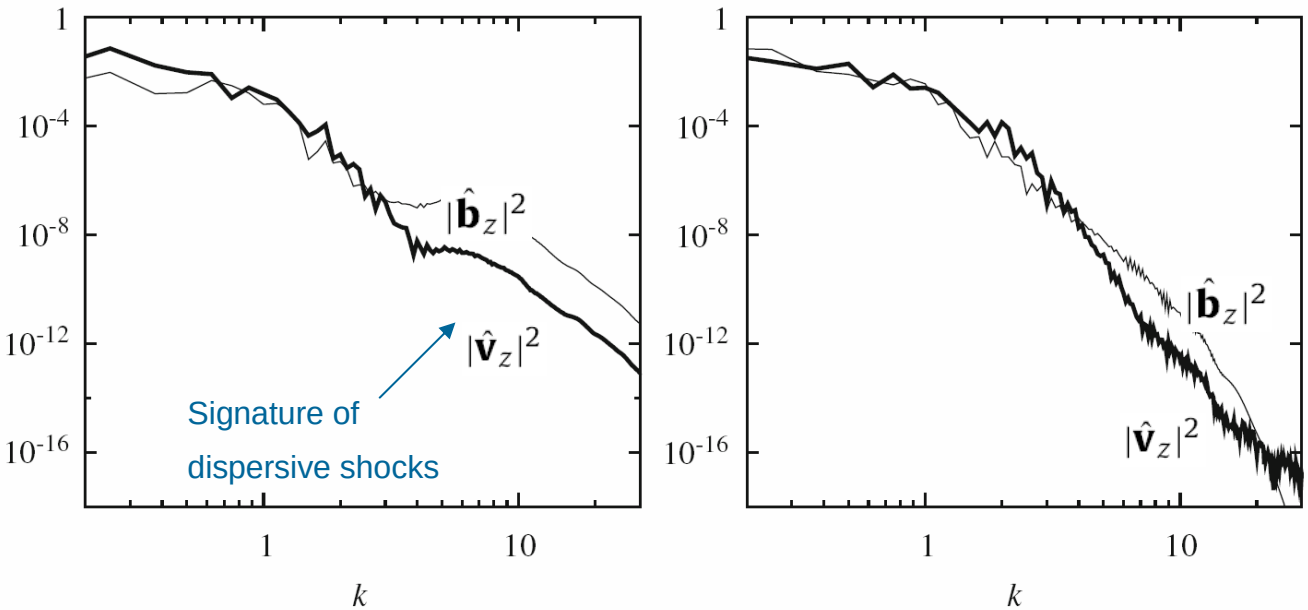


Locally averaged transverse kinetic and magnetic spectra near t=2500 and t=10500

Strong fluctuations of the energy spectra. Whistler modes are dominant.

Contrast with

Strongly dispersive regime (not shown): Kinetic Alfvén wave are significant

# ROLE OF TEMPERATURE ANISOTROPIES

# Terrestrial magnetosheath

Important role of the temperature anisotropy:

AIC (near quasi-perpendicular shock) and mirror instabilities (further inside magnetosheath)

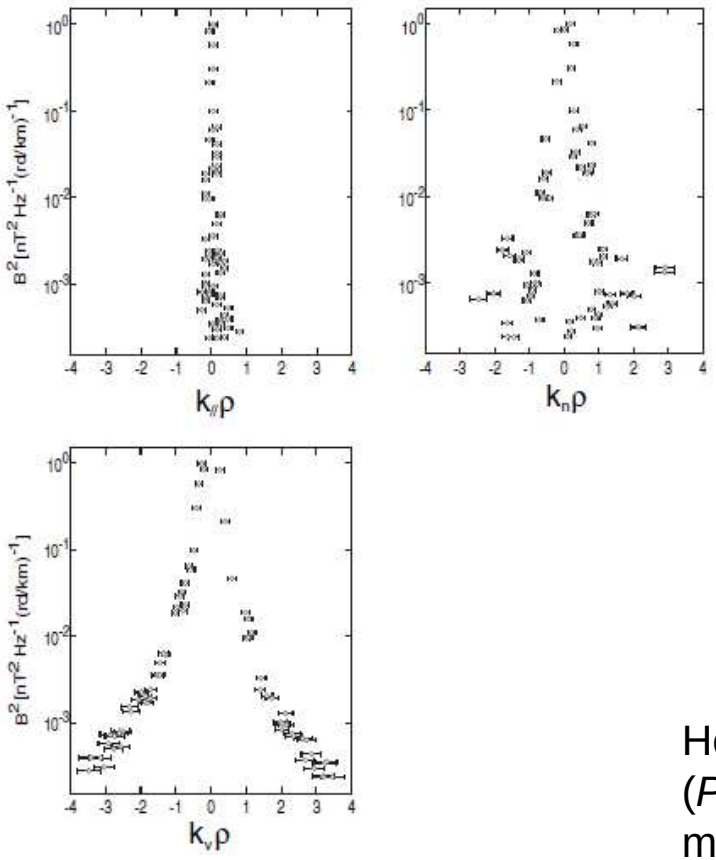


*Sahraoui et al. PRL 96, 075002 (2006)*

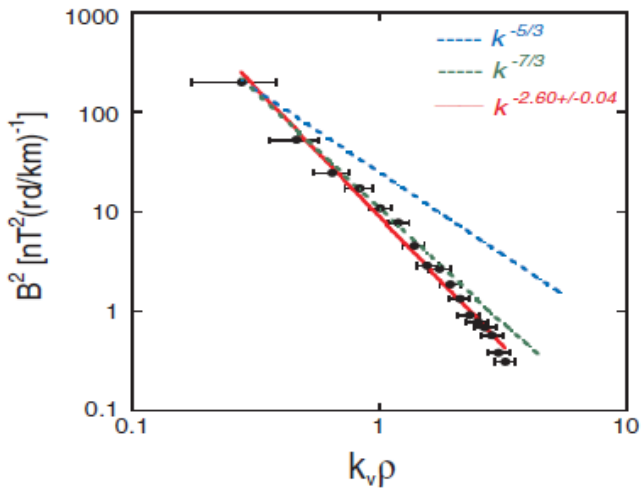


Domination of mirror modes

spatial spectrum steeper than temporal one

Here identified as mirror modes using k-filtering technique (*Pinçon & Lefeuvre, JGR 96, 1789; 1991*): modes with essentially zero frequency in the plasma frame

Anisotropy of fluctuations:

role of boundary conditions close to the magnetopause

Cascade preferentially along the flow direction

# Statistical study of temperature anisotropies

Turbulence (and/or solar wind expansion) generate temparature anisotropy
This anisotropy is limited by mirror and oblique firehose instabilities.
It seems to have some influence on the turbulence « dissipative range».

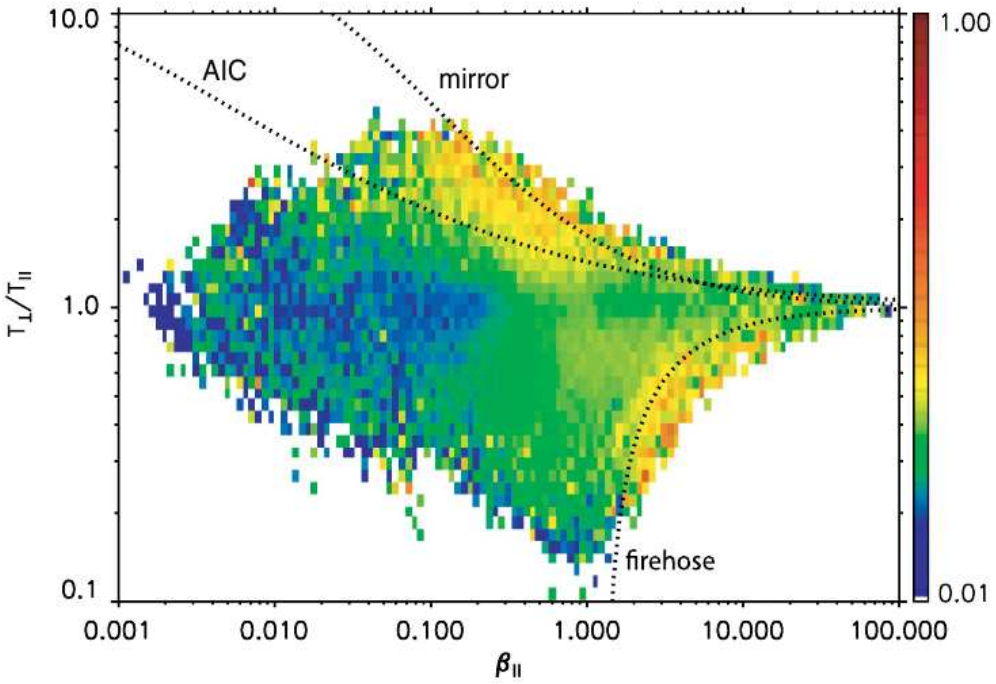


*Bale et al. PRL 103, 21101 (2009);*
*see also Hellinger et al. GRL* 33, L09101 (2006).

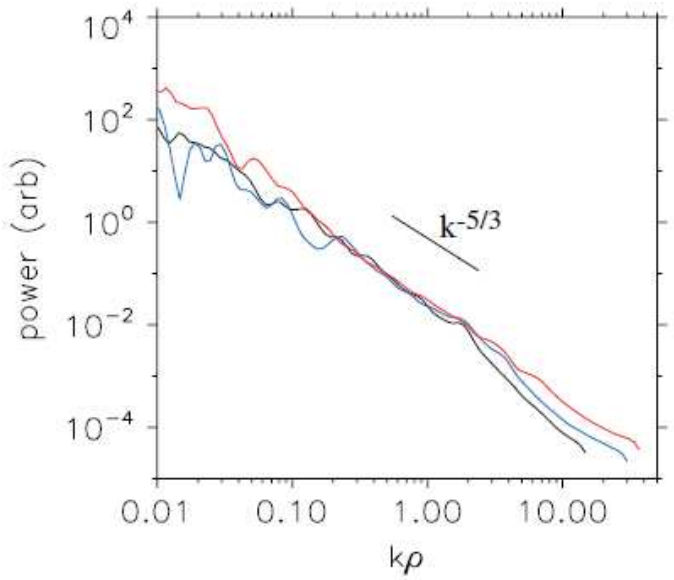


FIG. 4 (color). Wavelet power spectra of magnetic fluctuations at three different time intervals corresponding to perpendicular anisotropy $T_\perp/T_\parallel = 2.2$, $\beta_\parallel = 0.2$ (red trace), parallel anisotropy $T_\perp/T_\parallel = 0.5$, $\beta_\parallel = 1.9$ (blue trace), and isotropic protons $T_\perp/T_\parallel = 1$, $\beta_\parallel = 0.7$ (black trace). The spectra are plotted against $k\rho$ and have been scaled to the same average value over the interval $k\rho \in (0.2, 1.0)$, as described in the text. A solid black line with scaling $k^{-5/3}$ is shown. The interval above $k\rho \approx 1/2$ corresponds to the statistical data shown in Figs. 1 and 2.

# Goal

- Quantitative description of turbulent heating
- Characterization of the developing temperature anisotropy
- Analysis of resulting mirror instabilities and their feedback on the turbulent dynamics
- What kind of wave dominates?

## How to model turbulence in space plasmas?

3D Vlasov-Maxwell simulations are hardly possible on present-day computers.

Gyrokinetic simulations (*G. Howes PoP* ***15****, 055904 , 2008)* show the presence of cascades both in the physical and velocity spaces in the range $k_\perp \rho \geq 1$.

Applicability to space plasmas of the gyrokinetic theory (that concentrates on the quasi-transverse dynamics and average out the fast waves) is still to be validated.

One needs a model that allows for strong temperature anisotropies and that does not a priori orders out the fast magnetosonic waves.

## Landau fluids:

- Introduced by Hammett & Perkins (1990) as a closure retaining phase mixing and linear Landau damping.

- Implemented in the context of large-scale MHD dynamics by Snyder, Hammett & Dorland (1997) to close the hierarchy of moment equations derived from the drift kinetic equation.

- Extended to dispersive MHD by including FLR corrections computed perturbatively within the fluid formalism.
  (Goswami, Passot & Sulem 2005 and references within).

Landau-fluids are based on a full description of the hydrodynamic nonlinearities, supplemented by a linear (or quasi-linear) description of low-frequency kinetic effects (Landau damping and FLR corrections).

Fast waves are retained and accurately described up to (but not beyond) the ion gyroscale.

Landau fluids (and also gyrofluids) neglect wave particle trapping, i.e. the effect of particle bounce motion on the distribution function near resonance.

# Landau fluids

For the sake of simplicity, neglect electron inertia.

Ion dynamics: derived by computing velocity moments from Vlasov Maxwell equations.

$$\partial_t \rho_p + \nabla \cdot (\rho_p u_p) = 0$$

$$\partial_t u_p + u_p \cdot \nabla u_p + \frac{1}{\rho_p} \nabla \cdot \mathbf{p}_p - \frac{e}{m_p}(E + \frac{1}{c} u_p \times B) = 0$$

$$E = -\frac{1}{c}\left(u_p - \frac{j}{ne}\right) \times B - \frac{1}{ne} \nabla \cdot \mathbf{p}_e,$$

$$\partial_t B = -c \nabla \times E$$

$\rho_r = m_r n_r$

quasi-neutrality $(n_e = n_p)$

$$j = \frac{c}{4\pi} \nabla \times B$$

$\mathbf{p}_p = p_{\perp p}\mathbf{n} + p_{\parallel p}\boldsymbol{\tau} + \boldsymbol{\Pi}$, with $\mathbf{n} = \mathbf{I} - \widehat{b} \otimes \widehat{b}$ and $\boldsymbol{\tau} = \widehat{b} \otimes \widehat{b}$, where $\widehat{b} = B / |B|$.

Electron pressure taken gyrotropic (scales >> electron Larmor radius):
characterized by the parallel and transverse pressures $p_{\parallel e}$ and $p_{\perp e}$.

## For each particle species,

heat flux

Perpendicular and parallel pressures

$$\partial_t p_\perp + \nabla\cdot(u p_\perp) + p_\perp \nabla\cdot u - p_\perp \hat{b}\cdot\nabla u\cdot\hat{b} + \frac{1}{2}[\mathrm{tr}\ \nabla\cdot\mathbf{q} - \hat{b}\cdot(\nabla\cdot\mathbf{q})\cdot\hat{b}] = 0$$

$$\partial_t p_\parallel + \nabla\cdot(u p_\parallel) + 2p_\parallel \hat{b}\cdot\nabla u\cdot\hat{b} + \hat{b}\cdot(\nabla\cdot\mathbf{q})\cdot\hat{b} = 0$$

Equations for the parallel and perpendicular (gyrotropic) heat fluxes

$$\begin{cases} \partial_t q_\parallel + \nabla\cdot(q_\parallel u) + 3q_\parallel \widehat{b}\cdot\nabla u\cdot\widehat{b} + 3p_\parallel(\widehat{b}\cdot\nabla)\left(\frac{p_\parallel}{\rho}\right) + \nabla\cdot(\widetilde{r}_{\parallel\parallel}\widehat{b}) - 3\widetilde{r}_{\parallel\perp}\nabla\cdot\widehat{b} + \partial_z R_\parallel^{NG} = 0 \\ \partial_t q_\perp + \nabla\cdot(u q_\perp) + q_\perp\nabla\cdot u + p_\parallel(\widehat{b}\cdot\nabla)\left(\frac{p_\perp}{\rho}\right) + \frac{p_\perp}{\rho}\left(\partial_x\Pi_{xz} + \partial_y\Pi_{yz}\right) \\ \qquad + \nabla\cdot(\widetilde{r}_{\parallel\perp}\widehat{b}) + \left((p_\parallel - p_\perp)\frac{p_\perp}{\rho} - \widetilde{r}_{\perp\perp} + \widetilde{r}_{\parallel\perp}\right)(\nabla\cdot\widehat{b}) + \partial_z R_\perp^{NG} = 0 \end{cases}$$

Involve the 4 th rank gyrotropic cumulants $\widetilde{r}_{\parallel\parallel}$, $\widetilde{r}_{\parallel\perp}$, $\widetilde{r}_{\perp\perp}$

$$\widetilde{r}_{\parallel\parallel} = r_{\parallel\parallel} - 3\frac{p_\parallel^2}{\rho},$$

$$\widetilde{r}_{\parallel\perp} = r_{\parallel\perp} - \frac{p_\perp p_\parallel}{\rho},$$

$$\widetilde{r}_{\perp\perp} = r_{\perp\perp} - 2\frac{p_\perp^2}{\rho}.$$

$R_\parallel^{NG}$ and $R_\perp^{NG}$ stand for the nongyrotropic contribution of the fourth rank cumulants.

2 main problems:

(1) Closure relations are needed to express the 4th order cumulants $\widetilde{r}_{\parallel\parallel}, \widetilde{r}_{\parallel\perp}, \widetilde{r}_{\perp\perp}$
(closure at lowest order also possible, although usually less accurate)

(2) FLR corrections (non-gyrotropic) to the various moments are to be evaluated

The starting point for addressing these points is the linear kinetic theory in the low-frequency limit. $\omega/\Omega \sim \epsilon \ll 1$ Ω: ion gyrofrequency

For a unified description of fluid and kinetic scales, FLR-Landau fluids retain contributions of:

- quasi-transverse fluctuations $(k_\parallel/k_\perp \sim \epsilon)$ with $k_\perp r_L \sim 1$
- hydrodynamic scales with $k_\parallel r_L \sim k_\perp r_L \sim \epsilon.$ $r_L$: ion Larmor radius

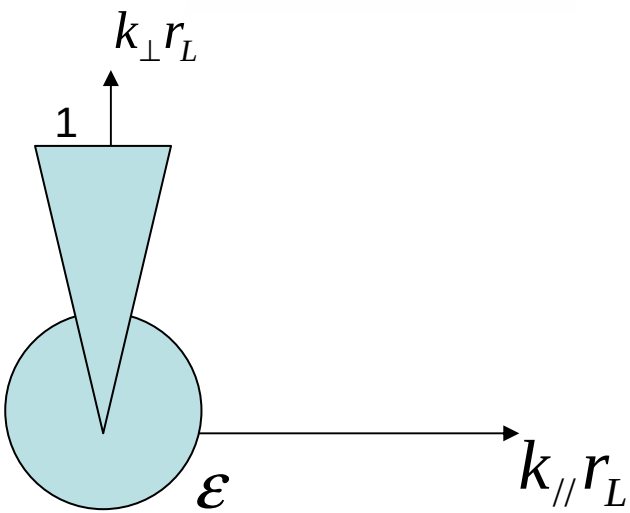

Closure relations are based on linearized kinetic theory (near a bi-Maxwellian distribution function) in the low frequency limit.

The dispersion function of the plasma is replaced by a Padé of suitable order, leading to linear PDEs for the 4th rank cumulants. For example:

$$\left(\frac{d}{dt} - 2|a_0|\sqrt{\frac{2T_\parallel^{(0)}}{m}}\mathcal{H}_z\partial_z\right)\tilde{r}_{\parallel\perp} + \frac{2T_\parallel^{(0)}}{m}\left(a_1 - \frac{1}{2}\right)$$
$$\times\partial_z\left[q_\perp + [\Gamma_0(b) - \Gamma_1(b)]\frac{p_\perp^{(0)}}{v_A^2}\left(\frac{T_\perp^{(0)} - T_\parallel^{(0)}}{m_p}\right)\frac{j_z}{en^{(0)}}\right] = 0.$$

Hilbert transform

replaced by instantaneous fields average

Similarly, the gyroviscous tensor is computed by combining various fluid quantities obtained from the linear kinetic theory, allowing to eliminate most occurrences of the plasma dispersion function.

Example;

$$\frac{1}{p_{\perp p}^{(0)}}\nabla_\perp\cdot\mathbf{\Pi}_\perp = -\nabla_\perp\mathcal{A} + \nabla_\perp\times(\mathcal{B}\hat{z}).$$

with

$$\mathcal{A} = \frac{1}{\Omega}\left[1 - \frac{\Gamma_1(b)}{b[\Gamma_0(b) - \Gamma_1(b)]} + \frac{\Gamma_1(b)}{\Gamma_0(b)}\right](\hat{z}\times i\vec{k}_\perp)\cdot\vec{u}_\perp$$
$$- \frac{1}{p_\perp^{(0)}}\frac{\Gamma_1(b)}{b\Gamma_0(b)}n^{(0)}\frac{r_L^2}{2}k_\perp^2 T_\perp.$$

T. Passot & P.L. Sulem, *Collisionless magnetohydrodynamics with gyrokinetic effects,* Phys. Plasmas, **14**, 082502 (2007)

Numerical Tests:

1. Diffusion of a temperature gradient
2. Dispersion relations of mirror modes and KAW

The code uses a pseudo-spectral method with Fourier series.

The time advance is performed using an Adams-Bashforth scheme.

No extra dissipation is added.

# Comparaison between Vlasov and Landau fluid simulations

## Diffusion of a temperature gradient

Vlasov (A. Mangeney and F. Califano)

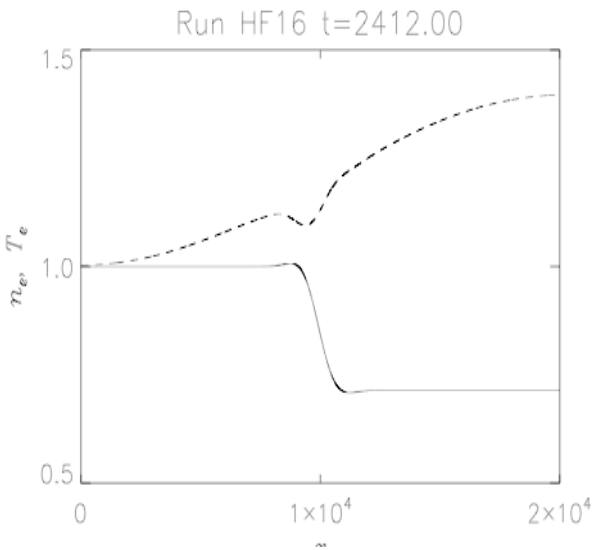


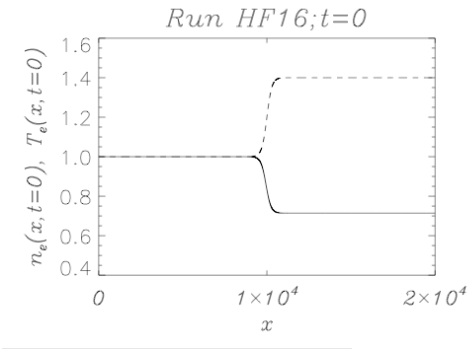


Initial condition

Domain size:
20 000 $\lambda_e$

Landau fluid

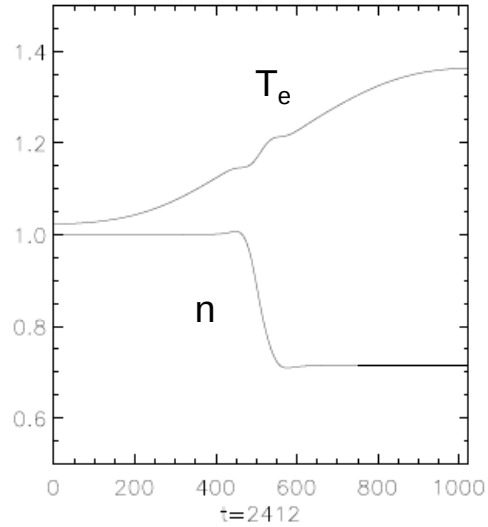


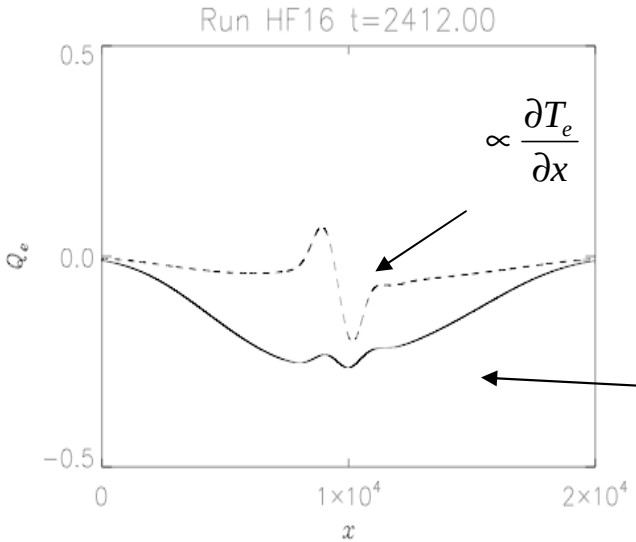


Parallel electron
heat flux

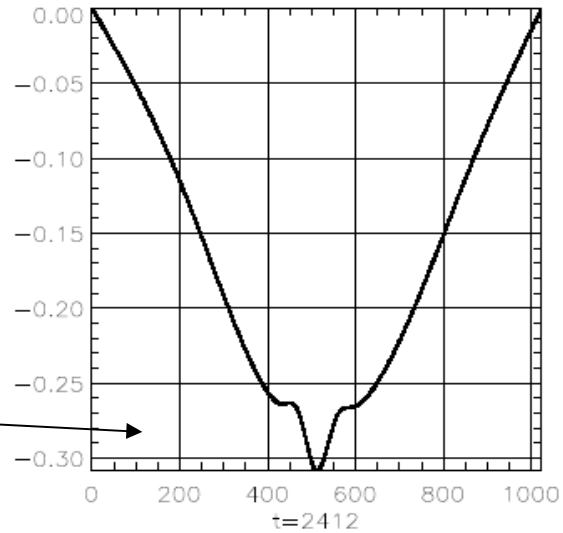

## Validation of the model by comparison with linear kinetic theory

# Mirror modes:

Normalized growth rate $\omega_i/\Omega_p$ versus $k_\perp r_L$

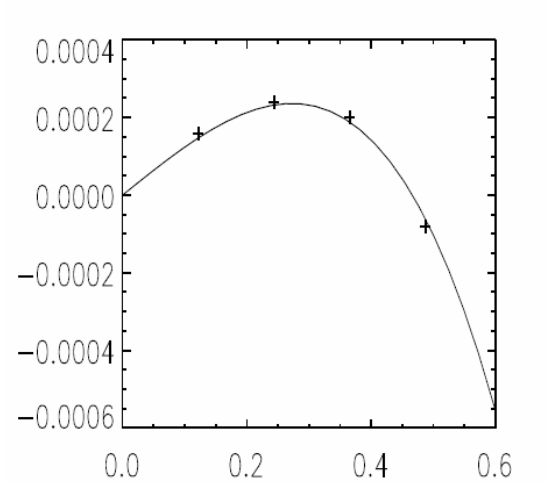


$\beta = 5,\ \tau = 0.1,\ \theta = \cos^{-1}(.1),$
$T_{\perp p}/T_{\parallel p} = 1.2$ and $T_{\perp e}/T_{\parallel e} = 1.$

$\tau = T_{\parallel e}/T_{\parallel p}$

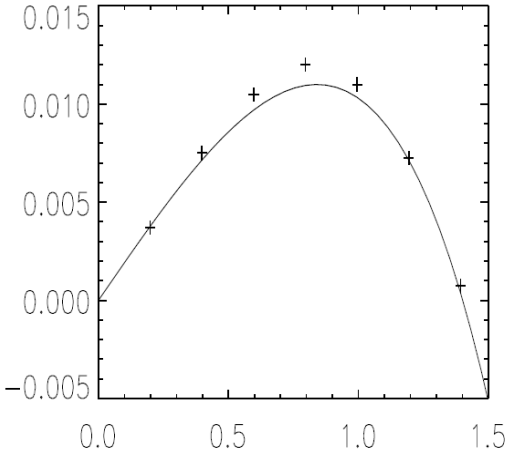


$\beta = 2,\ \tau = 1,\ \theta = \cos^{-1}(.1),$
$T_{\perp p}/T_{\parallel p} = 2$ and $T_{\perp e}/T_{\parallel e} = 1.$

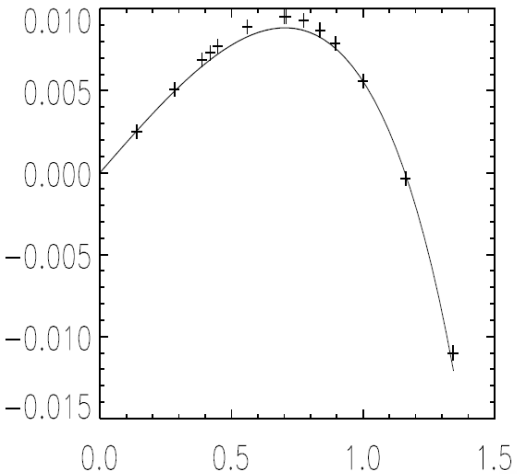


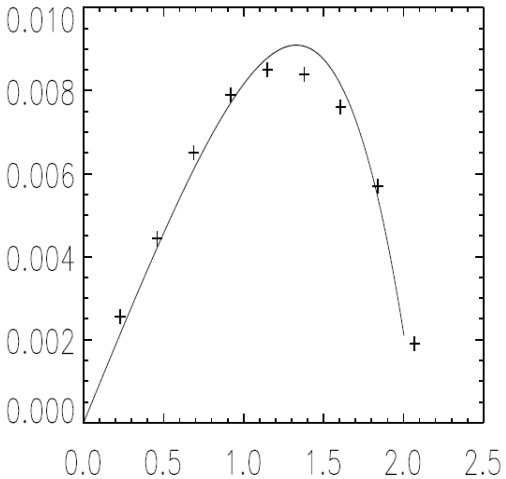


$\beta = 5,\ \tau = 1,\ \theta = \cos^{-1}(.2),$

$T_{\perp p}/T_{\parallel p} = 1.4$ and $T_{\perp e}/T_{\parallel e} = 1.$

$T_{\perp p}/T_{\parallel p} = 1.1$ and $T_{\perp e}/T_{\parallel e} = 1.18$

## Kinetic Alfvén waves:
### quasi-transverse propagation

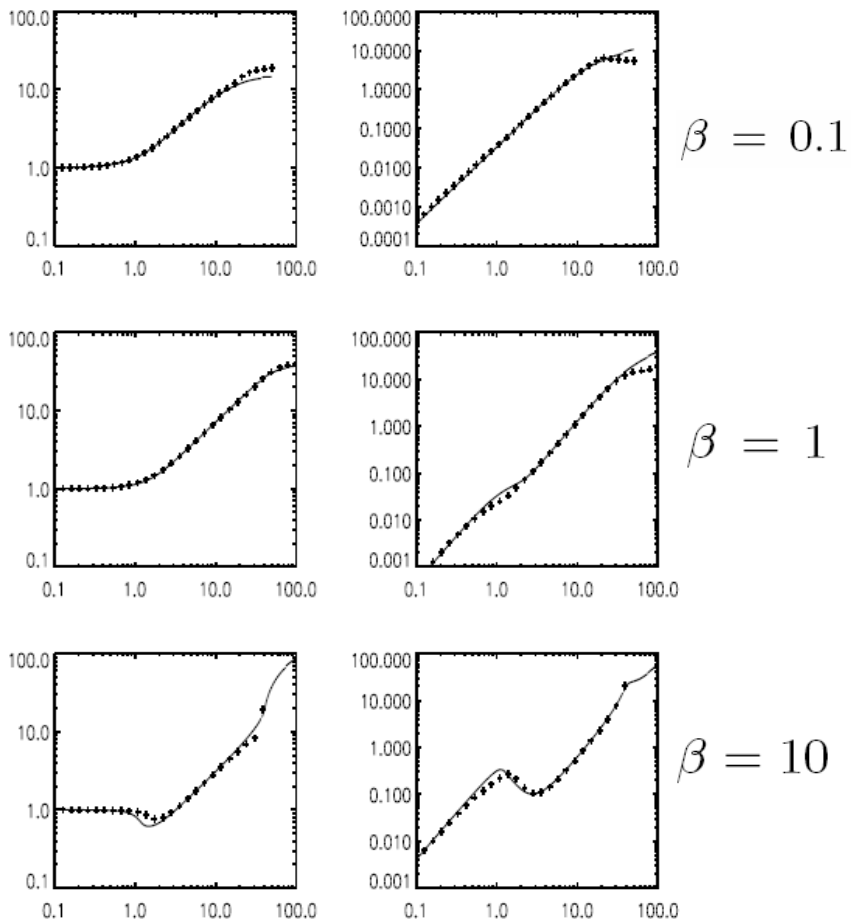


FIG. 2: Normalized frequency $\omega_r/(k_\parallel v_A)$ (left) and damping rate $-\omega_i/(k_\parallel v_A)$ (right) for KAWs with $\theta = \tan^{-1}(1000)$, $\tau = 1$, versus $k_\perp r_L$ for $\beta = 0.1$ (top), $\beta = 1$ (middle), $\beta = 10$ (bottom).

## Alfvén waves
### oblique propagation

Does not capture resonance

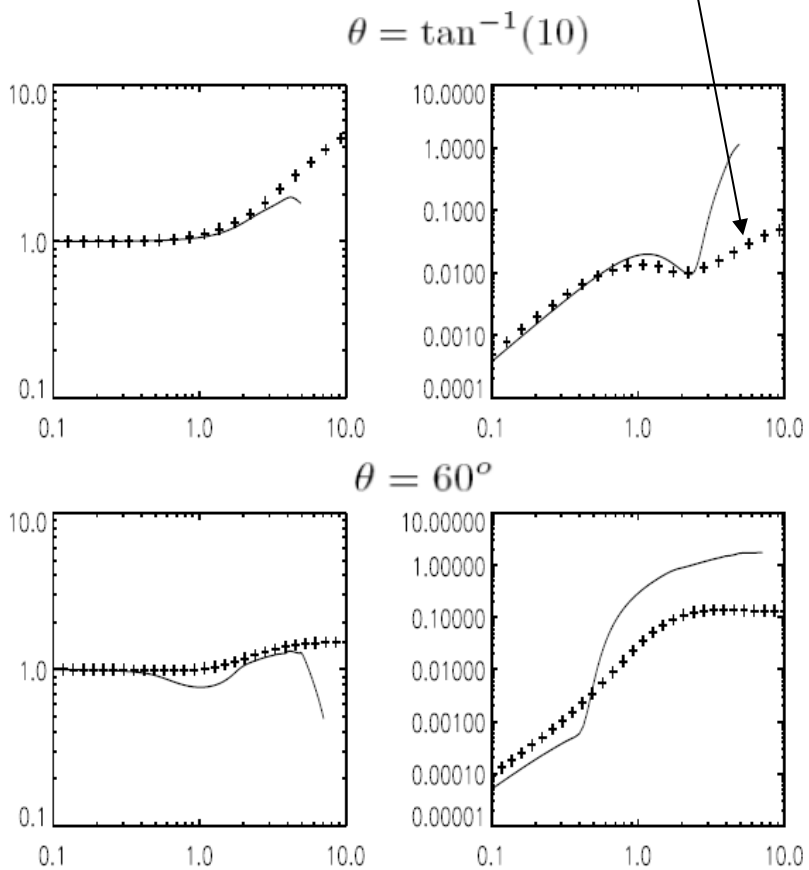


FIG. 3: Normalized frequency $\omega_r/(k_\parallel v_A)$ (left) and damping rate $-\omega_i/(k_\parallel v_A)$ (right) for KAWs with $\tau = 0.01$, $\beta = 1$ versus $k_\perp r_L$ for $\theta = \tan^{-1}(10)$ (top), $\theta = 60^o$ (bottom).

# Non-modal linear theory

The evolution of a small perturbation depends very much on the linear interactions between many different modes, including heavily damped ones.
This is especially important at kinetic scales.

In normal mode theory, the focus is on eigenmodes, which are assumed to grow or damp exponentially in time: attention is only paid to asymptotic in time behavior.

In non-modal theory, the initial value problem is solved, allowing transients.

Transients can be important when the linear operator is non-normal, i.e. does not commute with its adjoint.

Well kown effects in hydrodynamics
see e.g. Schmidt Ann. Rev. Fluid. Mech. (2007)

Eigenvectors are non-orthogonal.

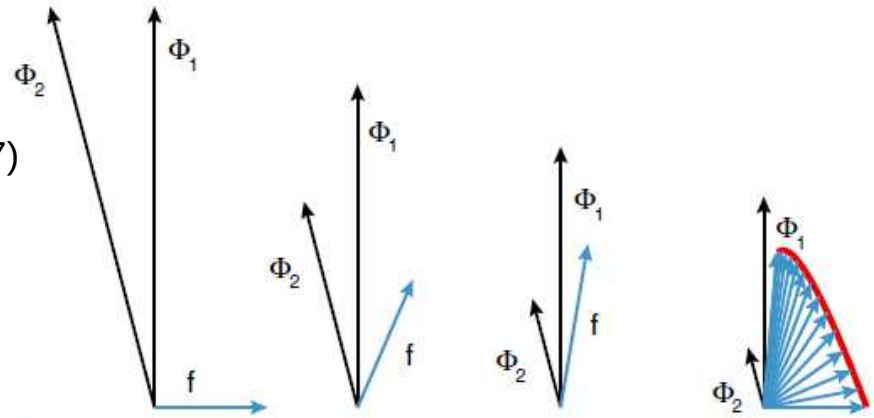


Figure 2

## The linearized LF equations is a non-normal system

(Camporeale et al. PoP **16**, 030703 (2009), ApJ **715**, 260 (2010)).

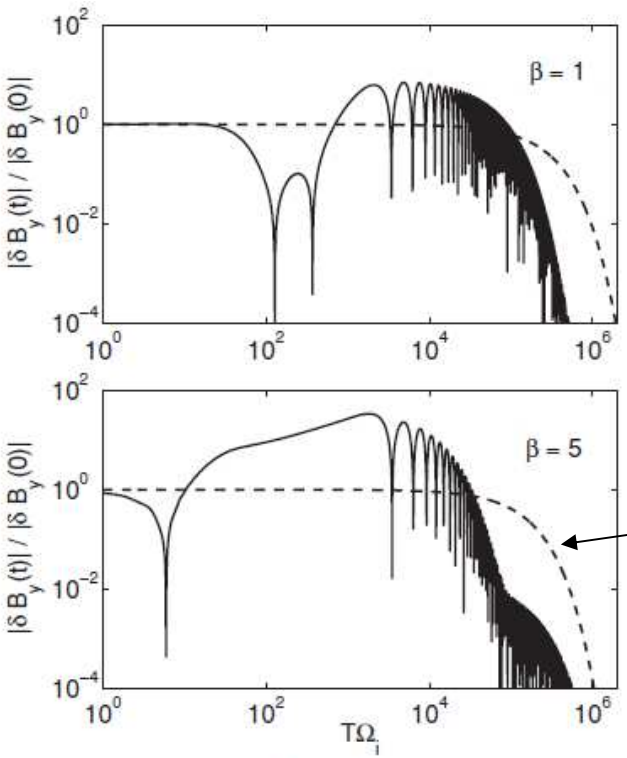


Prediction of modal theory.

**Figure 2.** Evolution in time of the absolute value of the amplitude of the $y$-component of the magnetic field, normalized to its initial value, for one particular choice of initial condition. The parameters used are: $k = 1$, $T_\perp/T_\parallel = 1$, and $\beta = 1$ (top panel) and $\beta = 5$ (bottom panel). The curve in dashed line is the evolution $e^{\alpha t}$, predicted by modal theory.

Remains amplified for a very long time

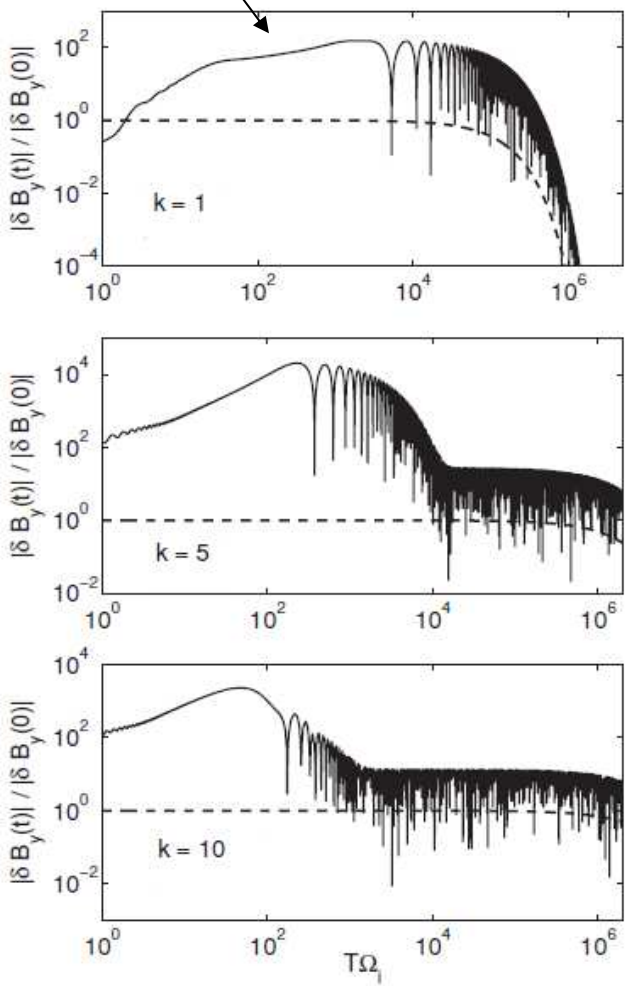


**Figure 3.** Evolution in time of the absolute value of the amplitude of the $y$-component of the magnetic field, normalized to its initial value, for one particular choice of initial condition. The parameters used are: $T_\perp/T_\parallel = 0.65$, $\beta = 5$, and $k = 1$ (top panel), $k = 5$ (central panel), and $k = 10$ (bottom panel). The curve in dashed line is the evolution $e^{\alpha t}$, predicted by modal theory.

Effect more important at larger values of beta and smaller scale

Average for 10 000 random initial perturbations

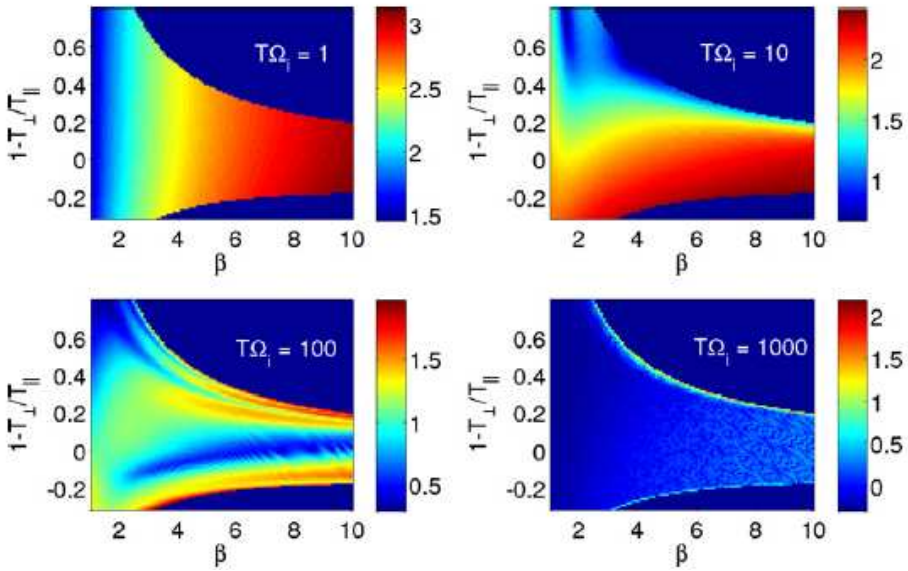


Total norm of state vector

Temperatures refer to electrons

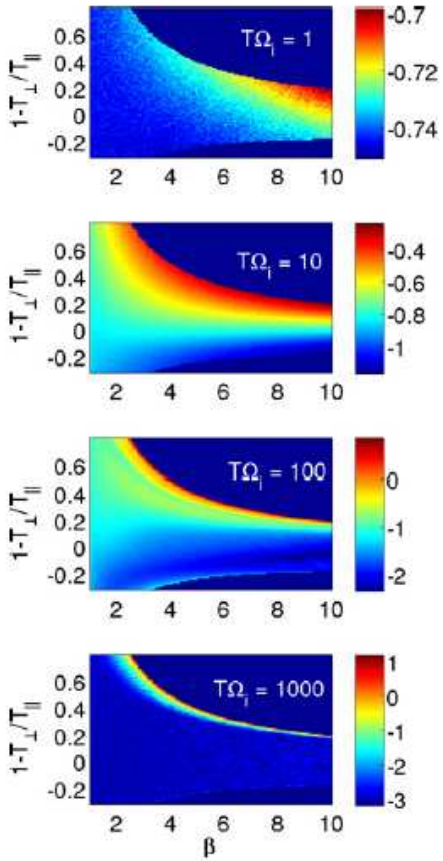


Magnetic fluctuation

Enhanced near stability boundary

In this scenario, a parcel of plasma could experience a “local” marginal stability condition due to a temporary enhanced magnetic fluctuation, and the anisotropy will be reduced in the same way as it is reduced under unstable conditions.

## Nonlinear simulations:

- A three-dimensional parallel code is developed in a simplified version (large-scale limit) (D. Borgogno, D. Laveder, P. Hunana) and starts to be used.

### Comparison between Landau fluid and hybrid PIC simulations

Propagation of an Alfvén wave in a density inhomogeneity (parallel high density channel)

Landau fluid

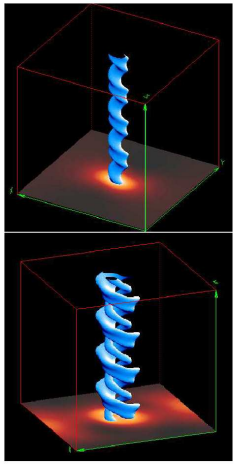

PIC

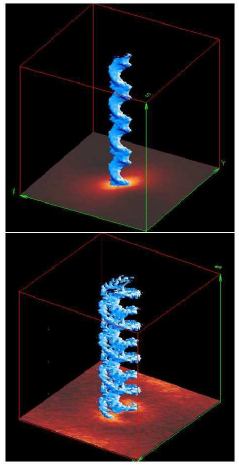

$$T_e / T_p = 1/30$$

$$\beta_p = 0.3 \quad \beta_e = 0.01$$

*(Borgogno et al. NPG **16**, 275 (2009))*

Project: simulation of turbulence in a collisionless magnetized plasma: evaluation of the dominant modes, cascade directions and heating rates.

Using the full model in 1D

# Mirror structures

from initial random noise $T_{//e}/T_{//p} = 0.05, \quad T_{\perp e}/T_{//e} = 1, \quad \cos\theta = 0.2$

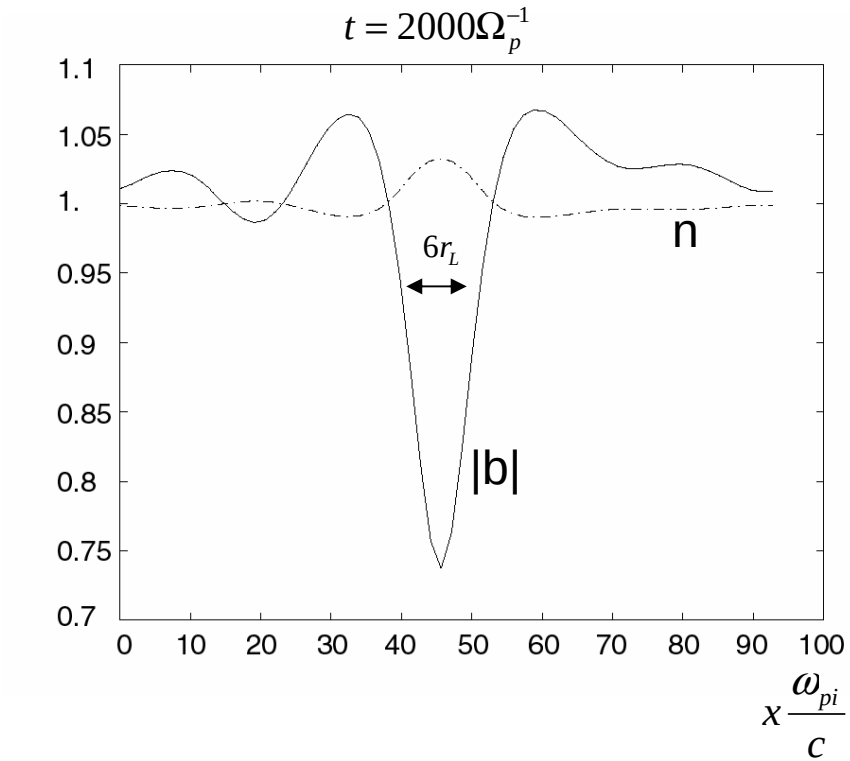


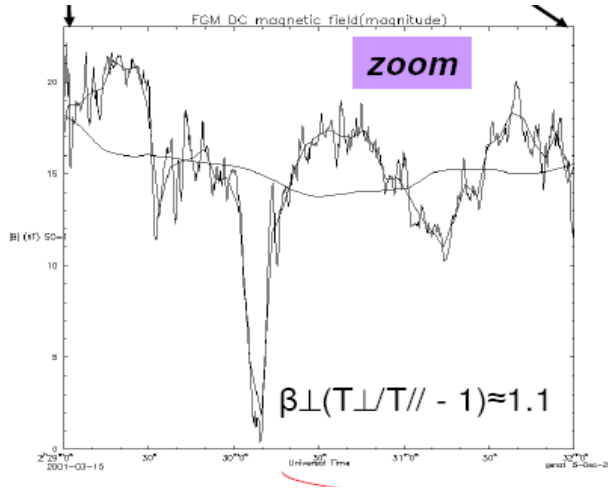


Cluster observations
(Génot et al.)

Formation of static magnetic holes

$$\beta_{//p} = 5, \quad T_{\perp p}/T_{//p} = 1.5$$

Does the mirror instability always lead to magnetic holes?

# Evidence of bistability

Stationary solution obtained by continuation below the threshold of mirror instability

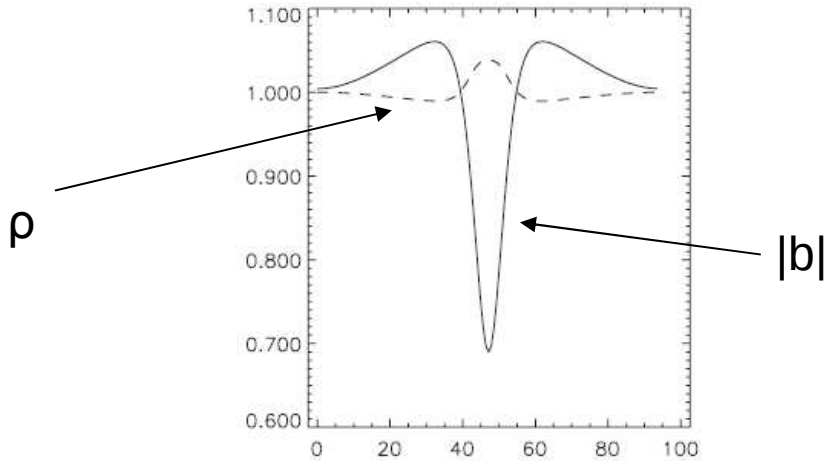


$\beta_{//p} = 5, \quad T_{\perp p} / T_{//p} = 1.25$ $\qquad \cos\theta = 0.2$ $\qquad T_{\perp e} = T_{\|e} = 0.05 T_{\|p}$

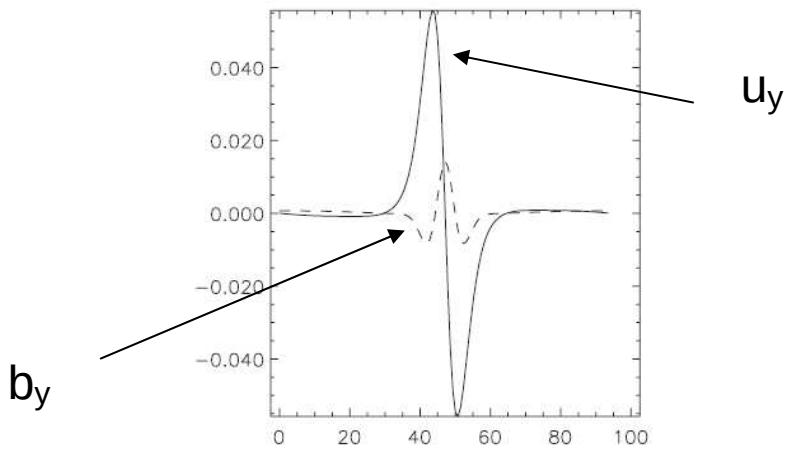


**Fig. 8.** Profiles of $u_y$ (solid) and $b_y$ (dashed) for the hole solution displayed in Fig. 6.

**Comment:**

Satellite observations:

Magnetic holes: mostly in subcritical regime

Magnetic humps: in supercritical regime (and large beta)

Structures observed in the terrestrial magnetosheath

*Génot et al., Ann. Geophys.* ***27,*** *601 (2009).*

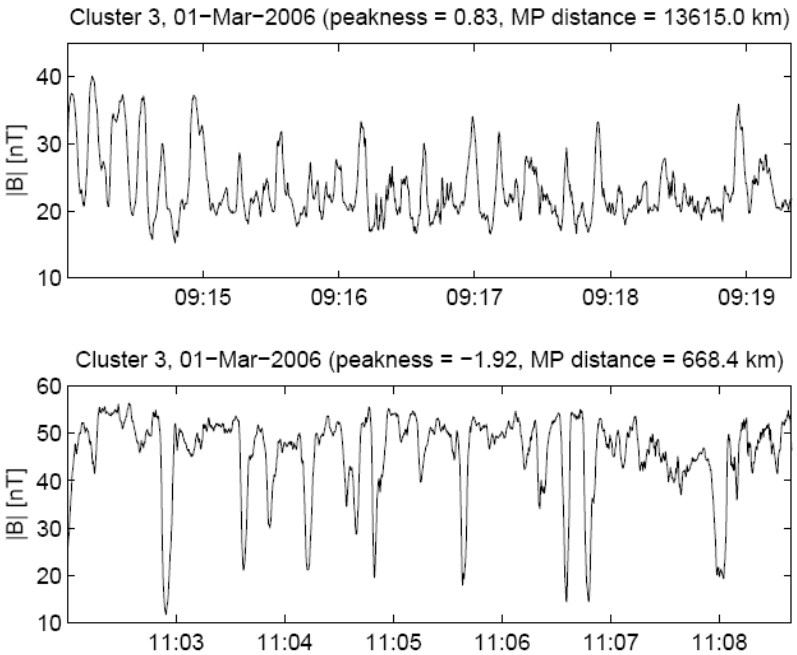


Soucek, Lucek & Dandouras JGR **113**, A04203 (2008)

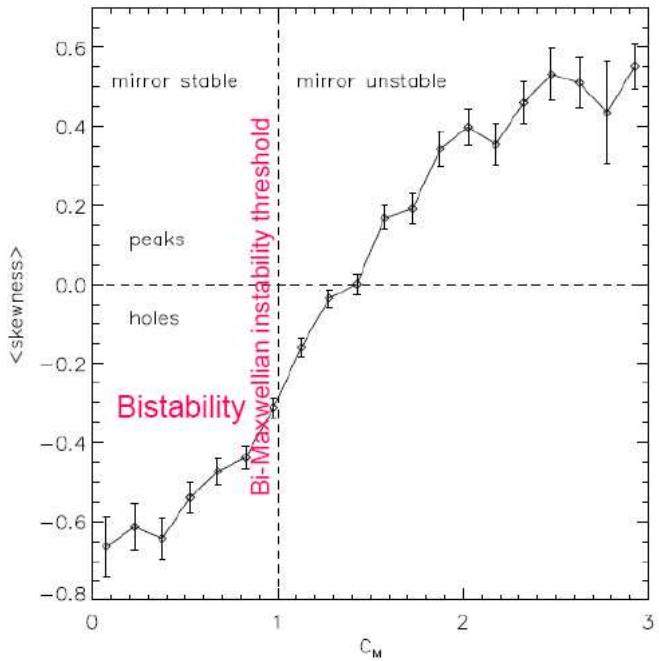


$$C_M = \beta_{p\perp}\left(\frac{T_{p\perp}}{T_{p\parallel}} - 1\right)$$

distance from threshold

Mirror instability that develops from small amplitude noise close to threshold leads to mirror humps in kinetic simulations.

⇨ The failure of the LF model to reproduce the formation of humps is associated to lack of quasilinear phase leading to plateau formation at $v_{//}=0$ (see Hellinger et al. GRL 2009).

With a PIC code in a large domain:
Domain size= 2048 $c/\omega_{pi}$
Growth rate: 0.005 Ωp
1024 cells with 500 000 particles/cell

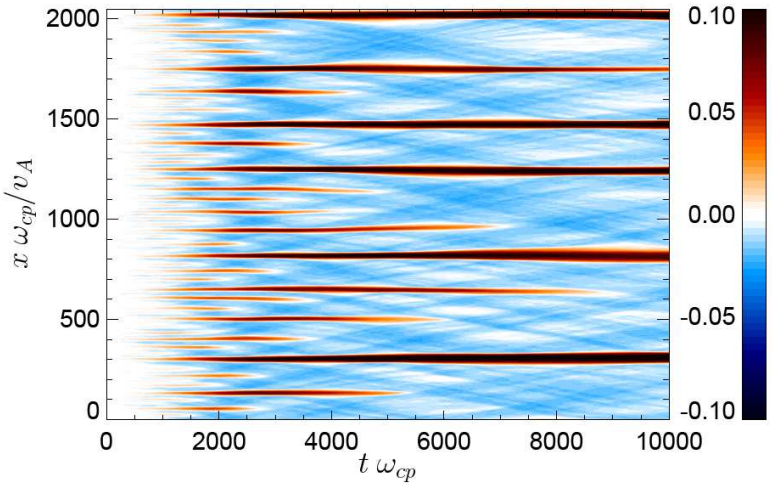


Color plot of the fluctuations of the magnetic field component $B_\eta$ perpendicular to the direction ζ of spatial variation, as a function of ζ and t.

*Califano et al., JGR 113, A08219 (2008).*

1D simulation:

$\theta_{kB} = 72.8°$ (most unstable direction)

$\beta_{p\|} = 1\ \beta_{p\perp} = 1.857 \quad \beta_e = 10^{-2}$

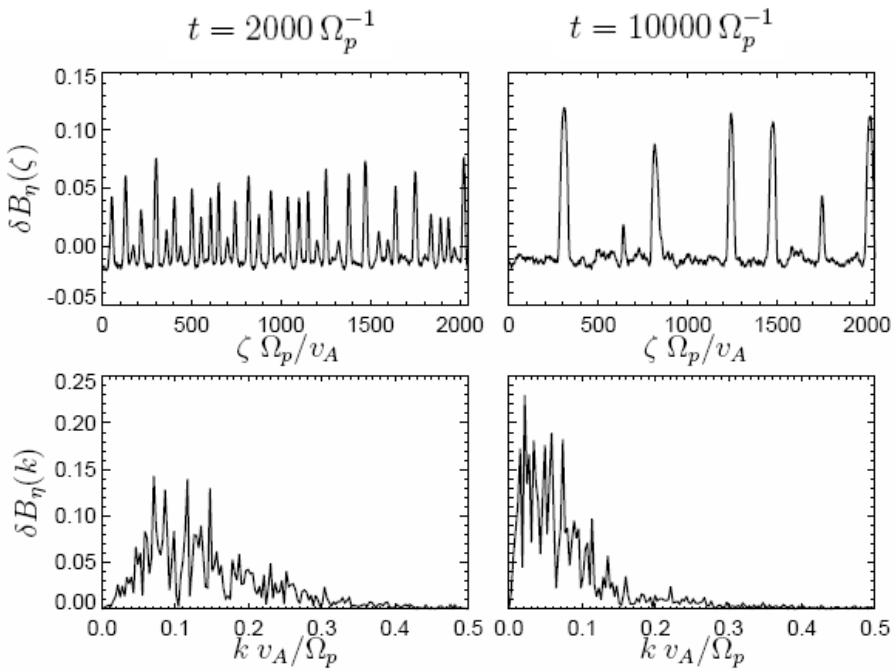


A large number of modes are excited.
Humps form and undergo coarsening.

# Vlasov-Maxwell simulation starting from large amplitude initial conditions

Subcritical solutions (i.e. below threshold)

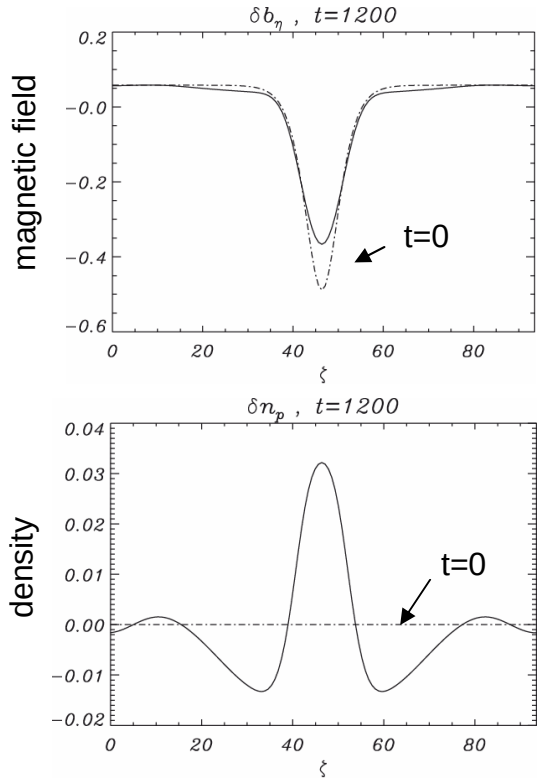


$$\beta_\parallel = 6, \quad \theta = 1.463, \quad T_\perp = T_\parallel$$

Large-amplitude magnetic holes survive even far **below and above threshold**.

Holes can also form after some time if starting far from onset.

A selection mechanism can possibly lead to predominant observation of holes.

The latter are thus expected to dominate in a turbulent environment.

Magnetic humps do not survive below threshold

# Landau fluid simulations of driven turbulence in 1D

- Angle of propagation: $80^o$ with respect to the ambiant magnetic field
- White noise in time random driving at $k_f d_i$=0.5 or 1, applied on the perpendicular velocity component ($u_y$) each time the kinetic energy falls below 0.05.
- Initial temperatures are isotropic with parallel proton $\beta$=0.6.
- The size of the domain is L=8π or 16 π in units of ion inertial length.

- Number of grid points: typically N=512.
- Dissipation: at each time step all the fields are filtered in Fourier space by multiplication with a steep *tanh* function centered at k=0.8*N/4

# Global evolution of the mean temperatures

$k_f d_i = 0.5$

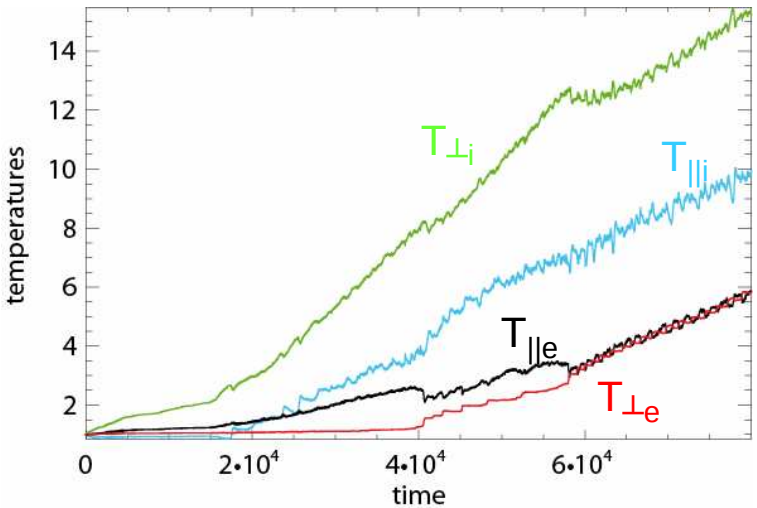


$k_f d_i = 1.$

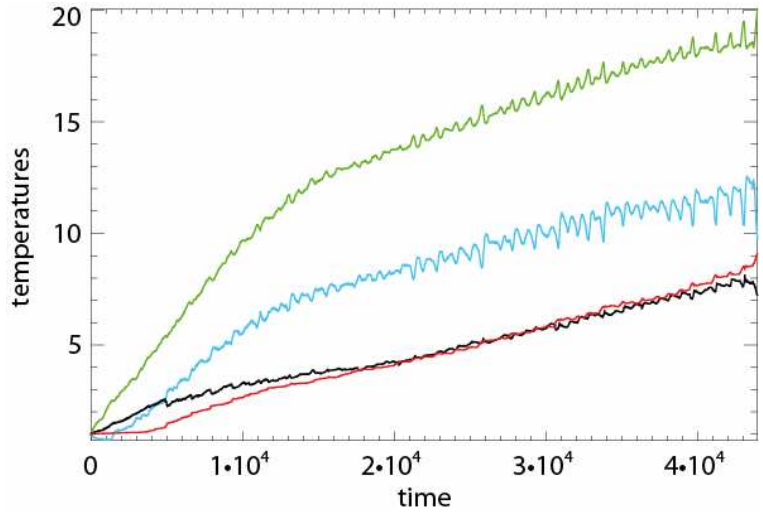


$L = 8\pi$

Perpendicular ion temperature

Parallel ion temperature

Parallel electron temperature

Perpendicular electron temperature

Growth of ion temperatures: with $T_\perp > T_{//}$

More moderate growth of electron temperature with $T_\perp < T_{//}$

This evolution contrasts with that associated with parametric decay of parallel propagating Alfvén waves for which the parallel (perpendicular) temperature is found to increase (decrease).

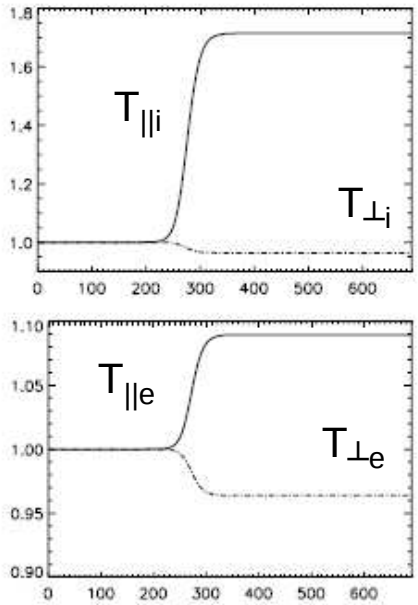


**Fig. 3.** Time evolution of parallel (solid lines) and transverse (dashed-dotted lines) mean temperatures of the ions (top) and the electrons (bottom) in the run of Fig. 1 (right).

Burgnon et al. **NPG** 11, 609 (2004)

The case of modulational instability is also different:

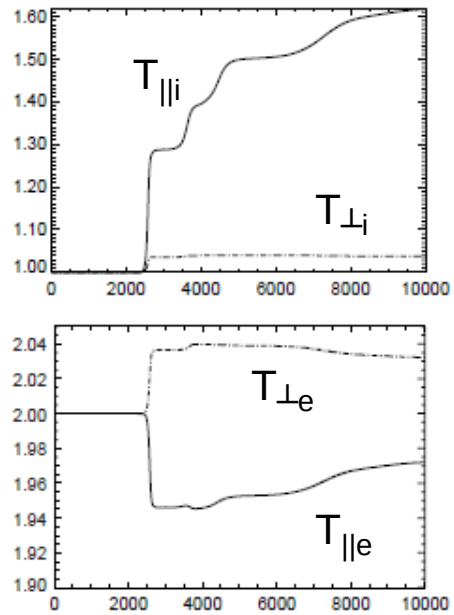


**Fig. 10.** Time evolution of parallel (solid lines) and transverse (dashed-dotted lines) of the ion (top) and electron (bottom) mean temperatures in the conditions of Fig. 7.

Results consistant with Hybrid PIC simulations of Matteini et al. JGR in press.

# Distance to mirror threshold

$k_f d_i = 0.5$

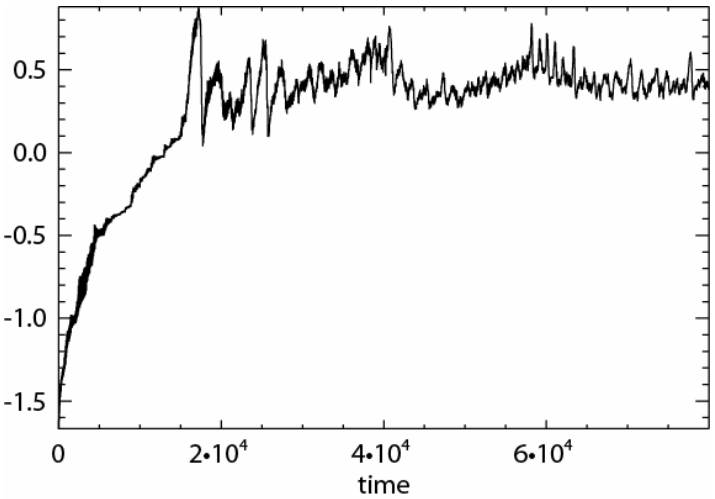


$k_f d_i = 1.$

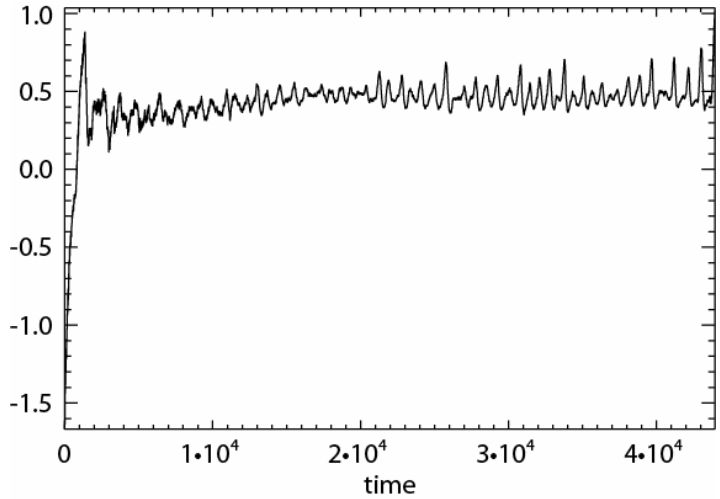


Mirror threshold in presence of hot anisotropic electrons in the long wavelength limit
(Pokhotelov et al. JGR 105, 2393 (2000))

$$\frac{T_{\perp i}}{T_{\parallel i}} - 1 + \frac{T_{\perp e}}{T_{\perp i}}\left(\frac{T_{\perp e}}{T_{\parallel e}} - 1\right) - \frac{T_{\parallel i} T_{\parallel e}}{2T_{\perp i}(T_{\parallel i} + T_{\parallel e})}\left(\frac{T_{\perp i}}{T_{\parallel i}} - \frac{T_{\perp e}}{T_{\parallel e}}\right)^2 - \beta_{\perp i}^{-1} = 0.$$

$k_f$=1.

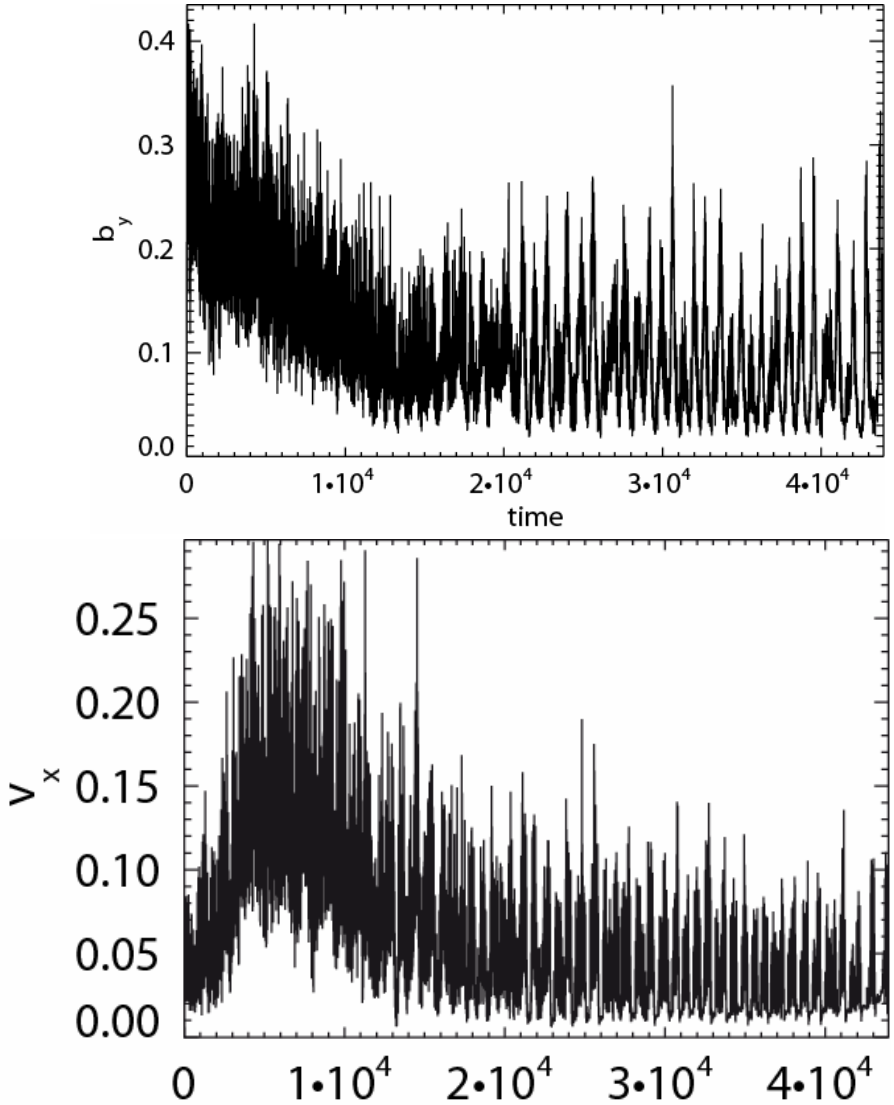


In the first phase, associated with a stronger heating and a growth of the nonlinearities, presence of **whistlers.**

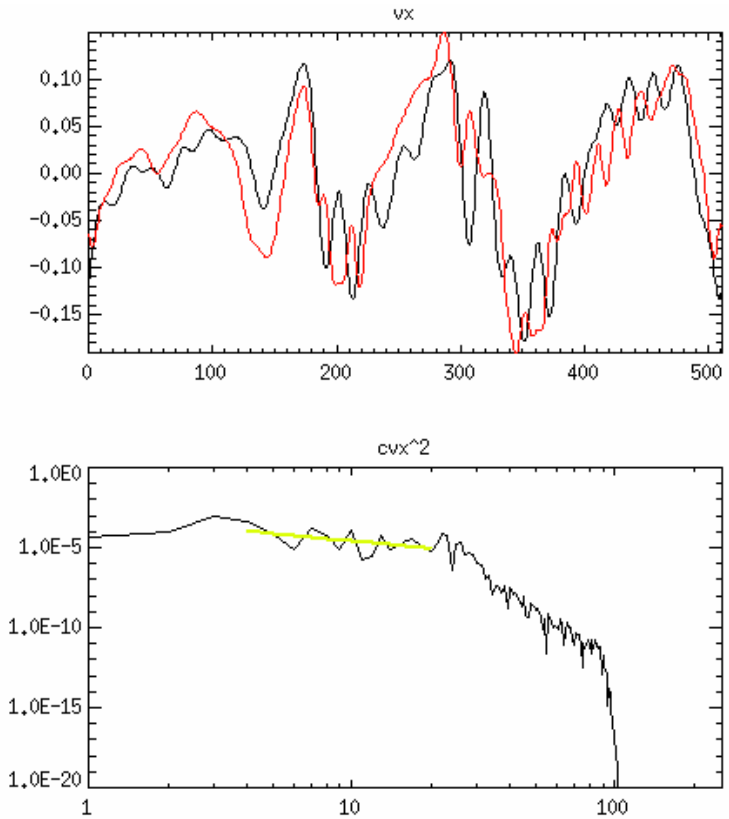

$k_f$=0.5

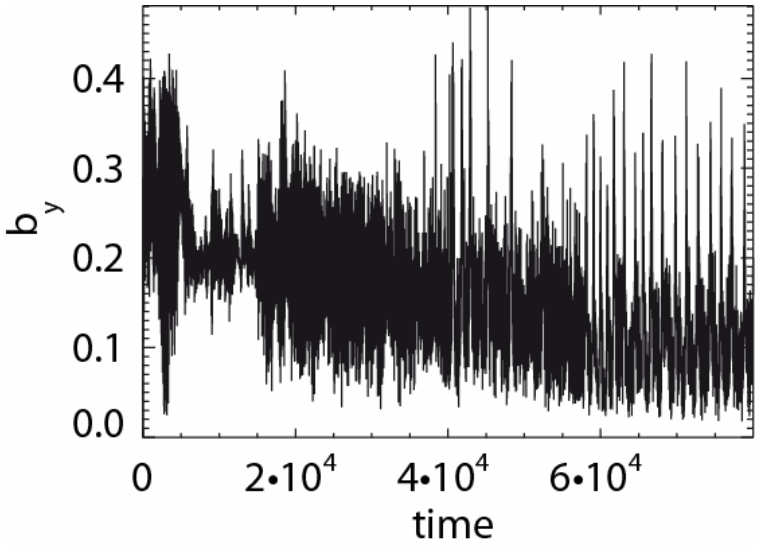


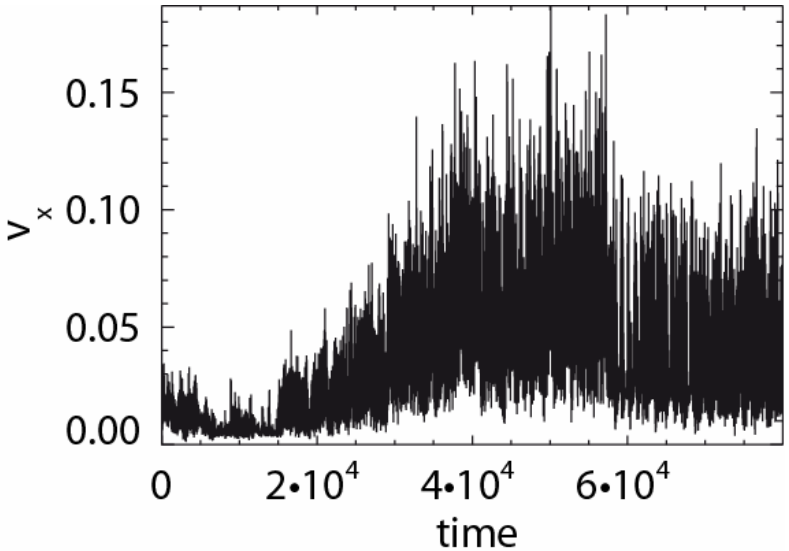


When forcing is at a larger scale, saturation is observed at longer time.

KAWs tend to be of much smaller amplitude in the mirror turbulence regime

# Mirror structures in a turbulent environment

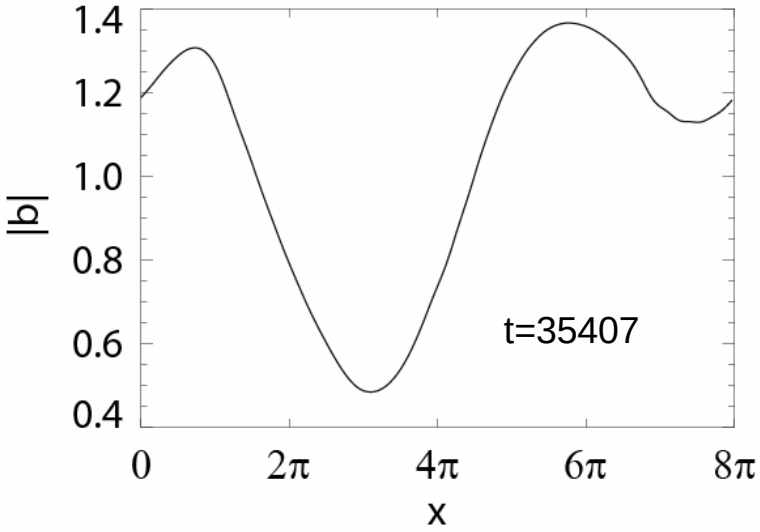


$k_f d_i$=0.5

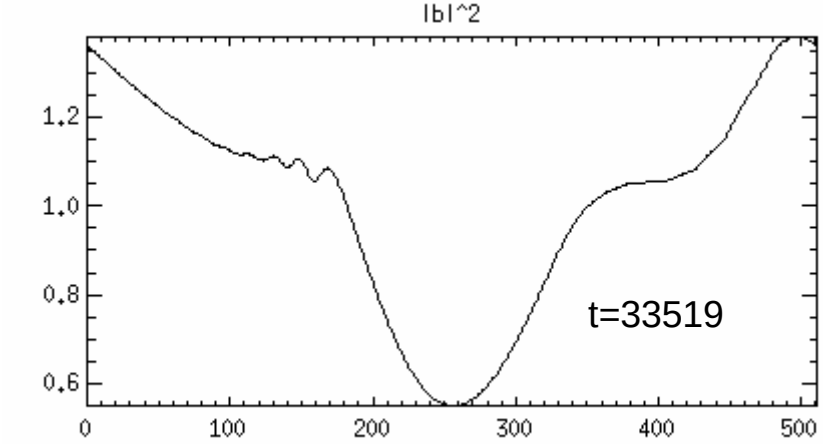


$k_f d_i$=1. t=5685

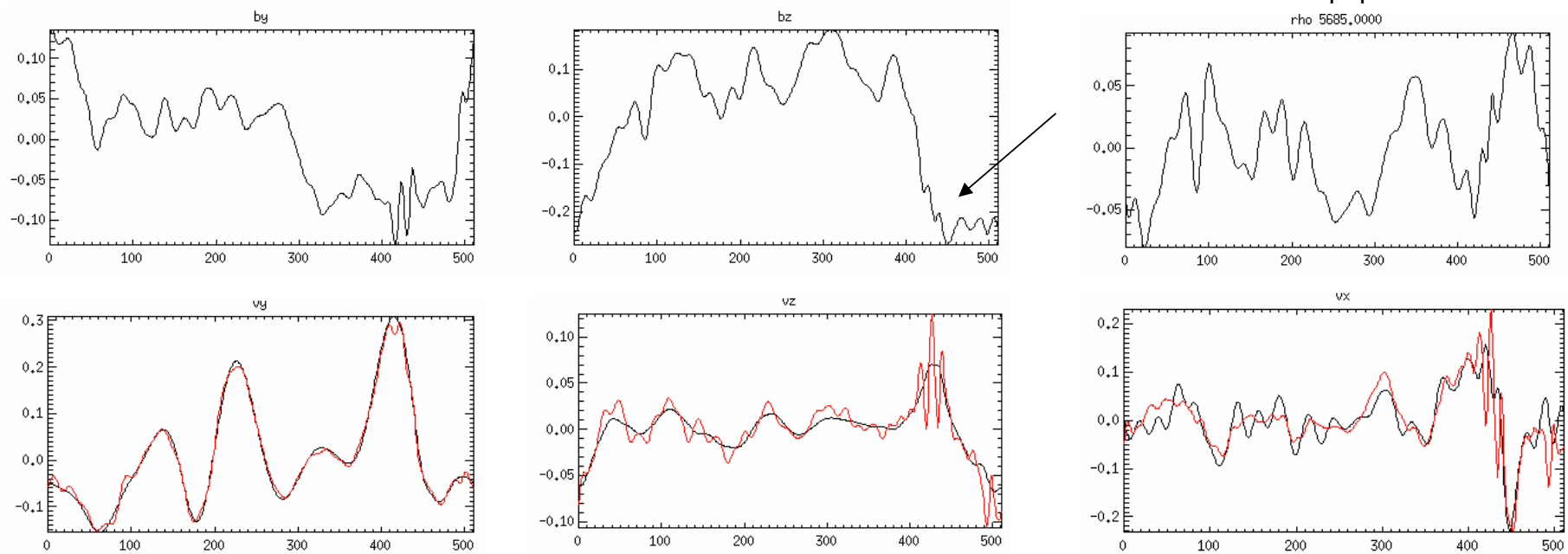


electron velocity

# Mirror structure with intermittent events

t=9306

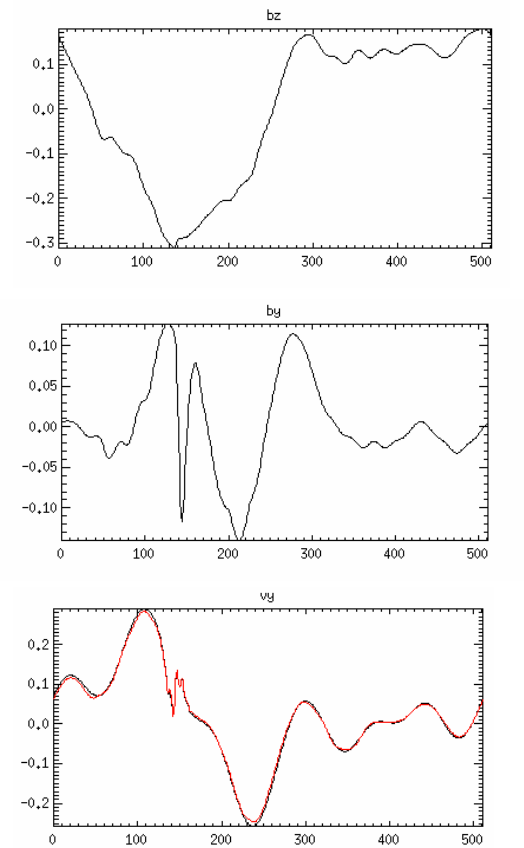


t=9326

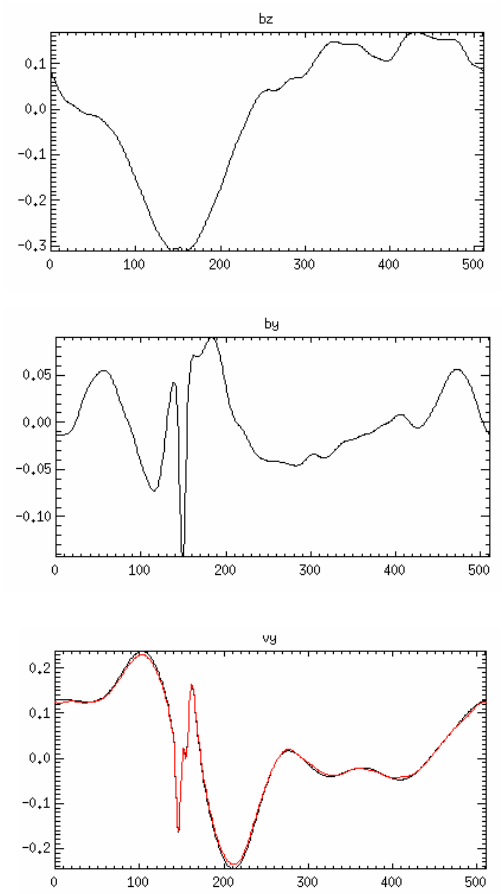


**These events are associated with a resonance phenomenon**
(propagation in an inhomogeneous medium)

## Mean parallel heat fluxes

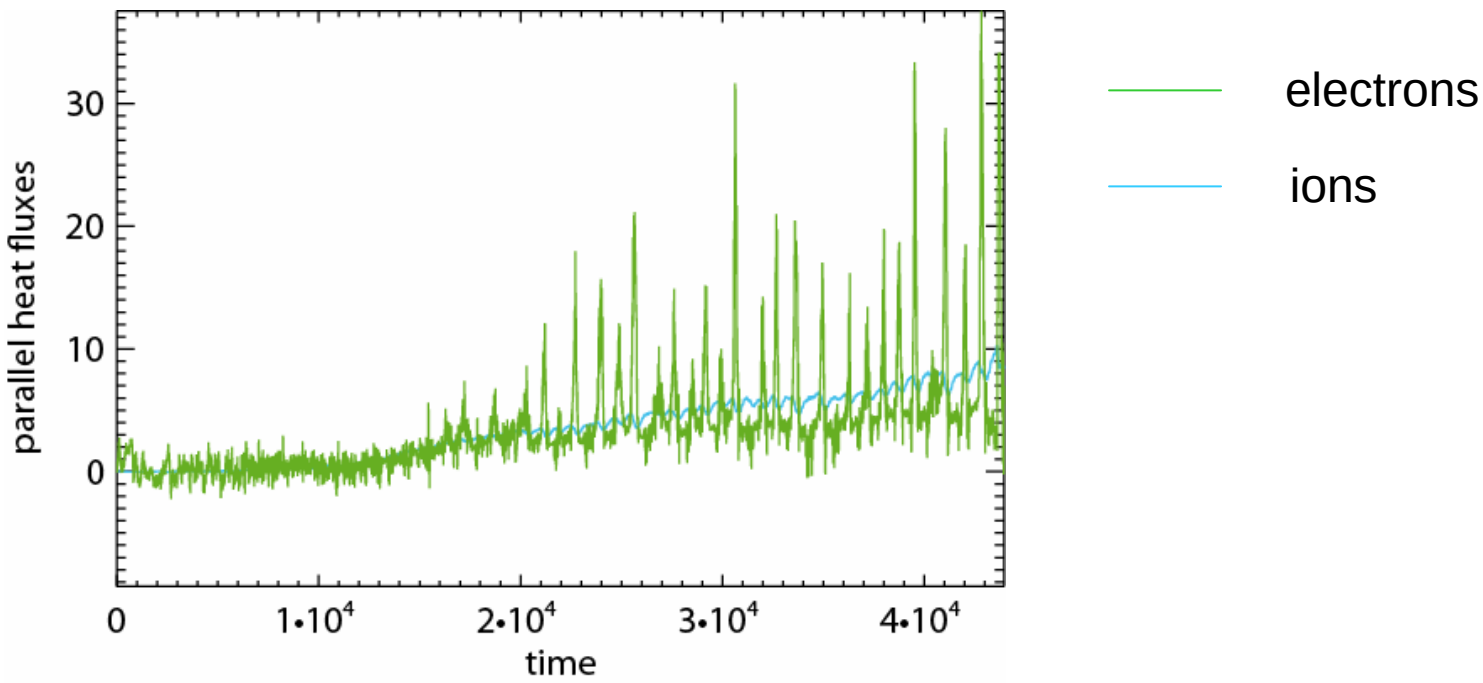


The intermittent events with large mean electron heat fluxes are associated with the growth of quasi-monochromatic waves.
These waves contribute to equalize parallel and perpendicular electron temperatures

Possibly slow waves

t=42805

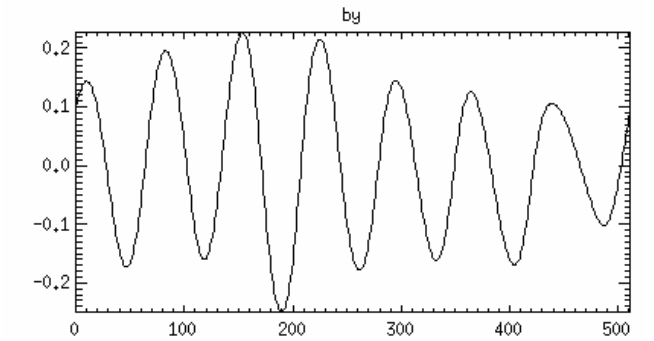


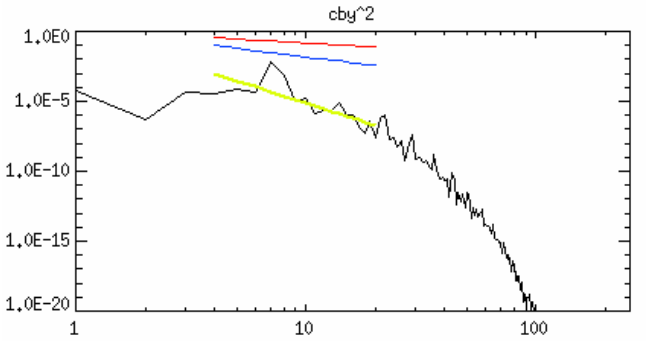


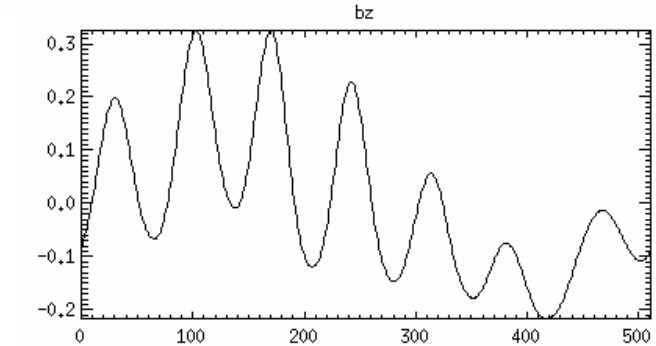


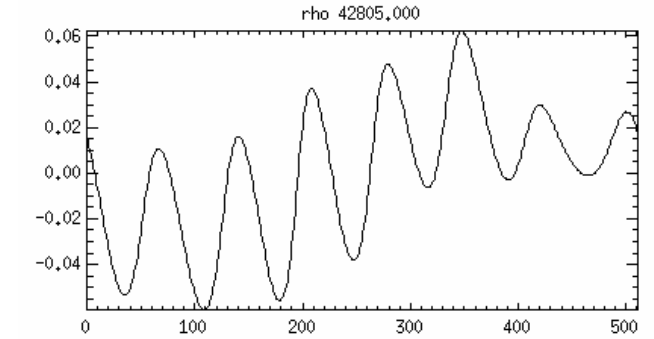


anticorrelation

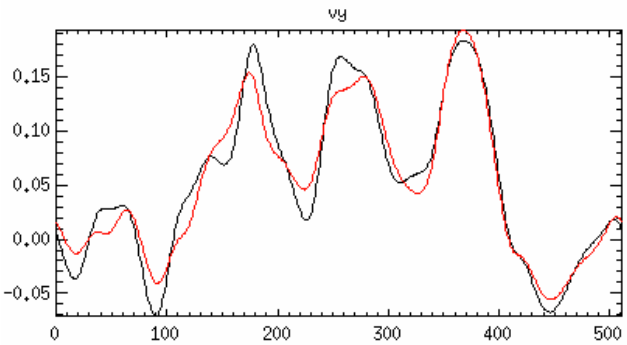


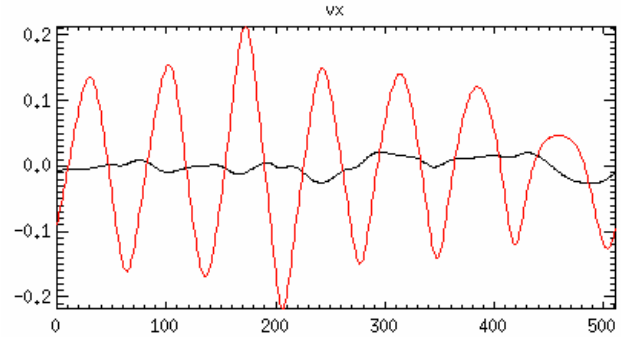


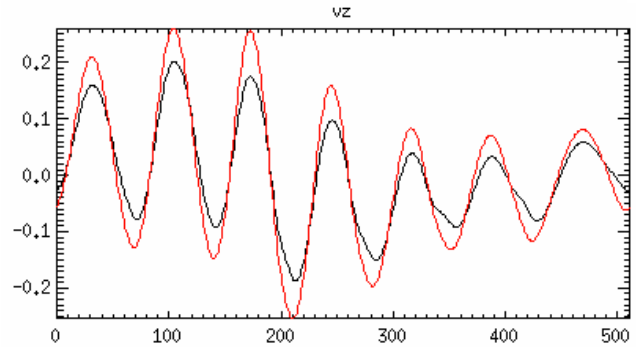

In a larger domain (L=16π) with large-scale driving results are similar.

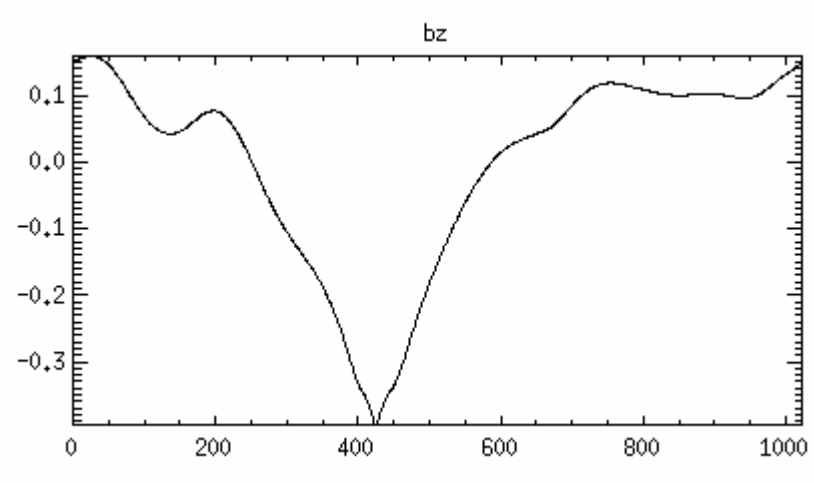


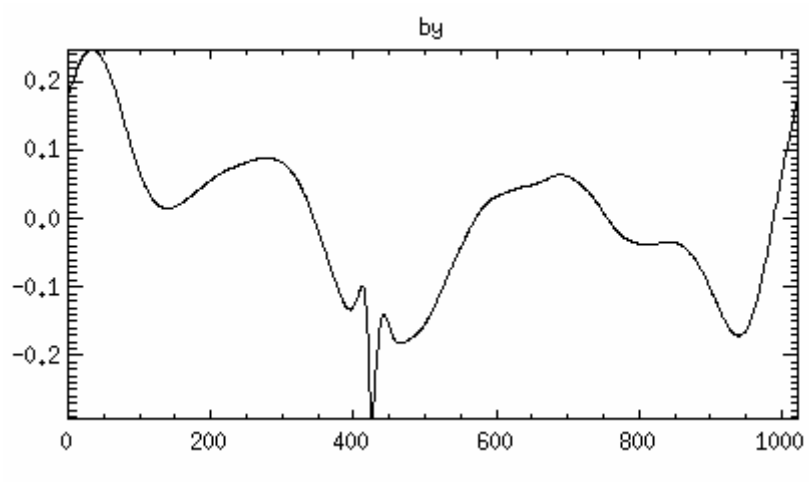


Width of the holes and wavelength of the generated wave remain unchanged

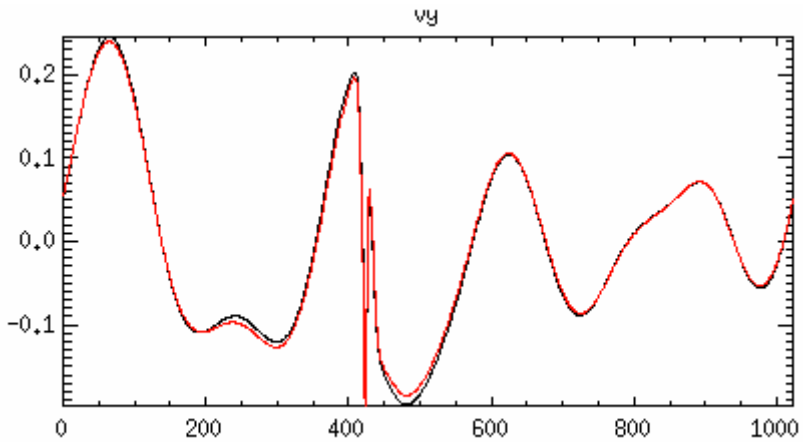


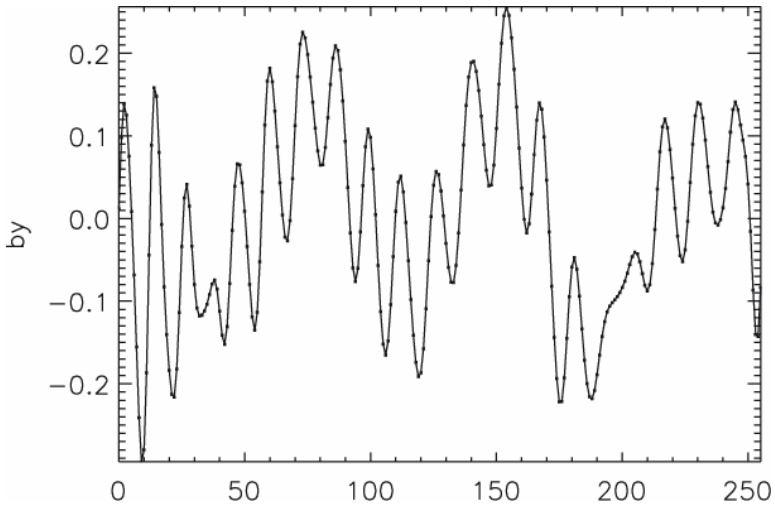

Assuming electrons are isothermal, the behavior is very different

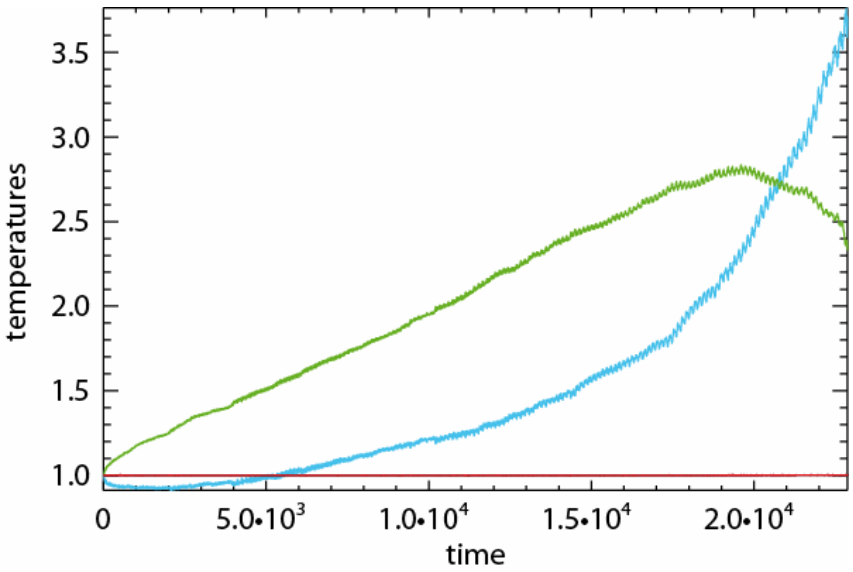


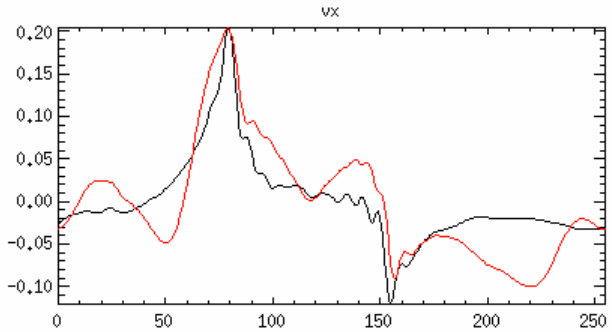


Solitary wave structure

No mirror mode

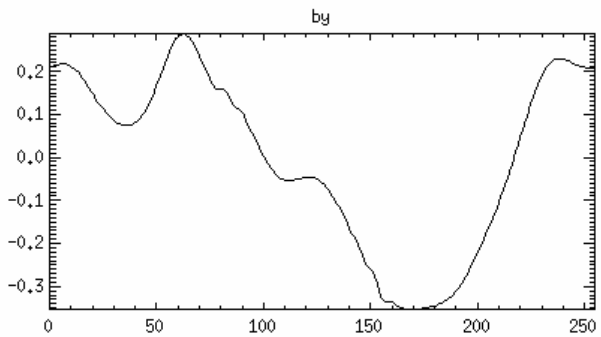


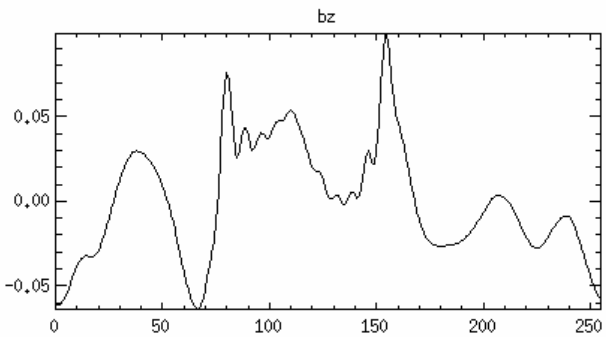


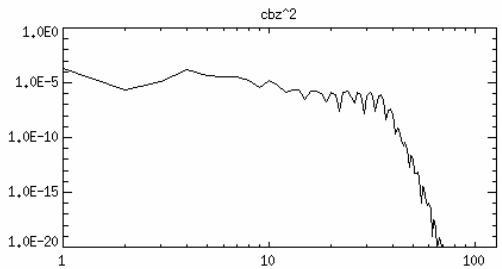


Electron Landau damping is absent, resulting in a shallower spectrum and a stronger heating for the parallel ion temperature

# SUMMARY

## Use of the FLR-Landau fluid model to study 1D oblique turbulence

- Temperature anisotropies are generated:
    - perpendicular ion temperature becomes larger than parallel ion temperature
    - electron temperatures undergo smaller growth with parallel temperature dominating the perpendicular one

- The growth of anisotropies is limited by the mirror instability for the ions.

- Parallel and perpendicular electron temperatures end up being equal in part due to the growth of large amplitude quasi-monochromatic waves.

- Mirror modes coexist with whistlers and KAWs. Very intermittent resonance effects are observed in the large gradients close to local minima of magnetic field amplitude.

- In the fully developed mirror turbulence regime, KAWs become subdominant.

- An isothermal model for the electrons does not reproduce this dynamics.